

Parameterized Approaches to Orthogonal Compaction^{*}

Walter Didimo^{a,1}, Siddharth Gupta^b, Philipp Kindermann^c,
 Giuseppe Liotta^a, Alexander Wolff^d, Meirav Zehavi^{e,2}

^a*Università degli Studi di Perugia, Perugia, Italy*

^b*BITS Pilani, K K Birla Goa Campus, Goa, India*

^c*Universität Trier, Trier, Germany*

^d*Universität Würzburg, Würzburg, Germany*

^e*Ben-Gurion University of the Negev, Beersheba, Israel*

Abstract

Orthogonal graph drawings are used in applications such as UML diagrams, VLSI layout, cable plans, and metro maps. We focus on drawing planar graphs and assume that we are given an *orthogonal representation* that describes the desired shape, but not the exact coordinates of a drawing. Our aim is to compute an orthogonal drawing on the grid that has minimum area among all grid drawings that adhere to the given orthogonal representation.

This problem is called orthogonal compaction (OC) and is known to be NP-hard, even for orthogonal representations of cycles [Evans et al. 2022]. We investigate the complexity of OC with respect to several parameters. Among others, we show that OC is fixed-parameter tractable with respect to the most natural of these parameters, namely, the number of *kitty corners* of the orthogonal representation: the presence of pairs of kitty corners in an orthogonal representation makes the OC problem hard. Informally speaking, a pair of kitty corners is a pair of reflex corners of a face that point at each other. Accordingly, the number of kitty corners is the number of corners that are involved in some pair of kitty corners.

^{*}A preliminary version of this paper appeared in the proceedings of SOFSEM 2023.

Email addresses: walter.didimo@unipg.it (Walter Didimo),
siddharthg@goa.bits-pilani.ac.in (Siddharth Gupta), kindermann@uni-trier.de
 (Philipp Kindermann), giuseppe.liotta@unipg.it (Giuseppe Liotta),
meiravze@bgu.ac.il (Meirav Zehavi)

¹Work partially supported by Dept. Engineering, Università degli Studi di Perugia, grant RICBA21LG: Algoritmi, modelli e sistemi per la rappresentazione visuale di reti.

²Work partially supported by European Research Council (ERC) grant PARAPATH.

Keywords: Orthogonal Graph Drawing, Orthogonal Representation, Compaction, Parameterized Complexity

1. Introduction

In a *planar orthogonal drawing* of a planar graph G each vertex is mapped to a distinct point of the plane and each edge is represented as a sequence of horizontal and vertical segments. A planar graph G admits a planar orthogonal drawing if and only if it has vertex-degree at most four. A *planar orthogonal representation* H of G is an equivalence class of planar orthogonal drawings of G that have the same “shape”, i.e., the same planar embedding, the same ordered sequence of bends along the edges, and the same vertex angles. A planar orthogonal drawing belonging to the equivalence class H is simply called a *drawing of H* . For example, Figs. 1a and 1b are drawings of the same orthogonal representation, while Fig. 1c is a drawing of the same graph with a different shape.

Given a planar orthogonal representation H of a connected planar graph G , the *orthogonal compaction* problem (OC for short) for H asks to compute a minimum-area drawing of H . More formally, it asks to assign integer coordinates to the vertices and to the bends of H such that the area of the resulting planar orthogonal drawing is minimum over all drawings of H . The area of a drawing is the area of the minimum bounding box that contains the drawing. For example, the drawing in Fig. 1a has area $7 \times 5 = 35$, whereas the drawing in Fig. 1b has area $7 \times 4 = 28$, which is the minimum for that orthogonal representation.

The area of a graph layout is considered one of the most relevant readability metrics in orthogonal graph drawing (see, e.g., [1, 2]). Compact grid drawings are desirable as they yield a good overview without neglecting details. For this reason, the OC problem is widely investigated in the literature. Bridgeman et al. [3] showed that OC can be solved in linear time, in the number of vertices and bends, for a subclass of planar orthogonal representations called *turn-regular*. Informally speaking, a face of a planar orthogonal representation H is turn-regular if it does not contain any pair of so-called *kitty corners*, i.e., a pair of reflex corners (turns of 270°) that point to each other; a representation is turn-regular if all its faces are turn-regular. See Fig. 1 and refer to Section 2 for a formal definition. On the other hand, Patrignani [4] proved that, unfortunately, OC is NP-hard in general. Evans et al. [5] showed that OC

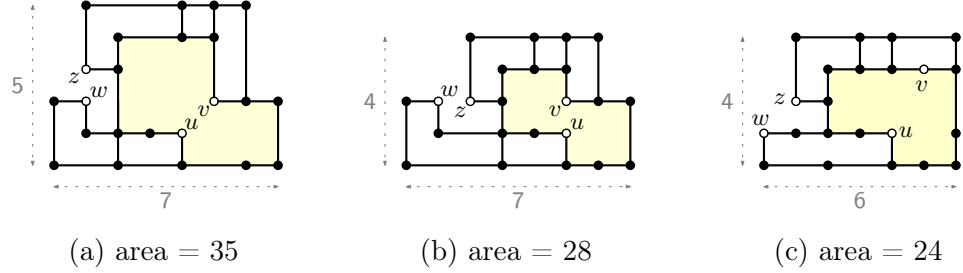


Figure 1: (a) Drawing of a non-turn-regular orthogonal representation H ; vertices u and v point to each other in the filled internal face, thus they represent a pair of kitty corners. Vertices w and z are a pair of kitty corners in the external face. (b) Another drawing of H with minimum area. (c) Minimum-area drawing of a turn-regular orthogonal representation of the same graph.

remains NP-hard even for orthogonal representations of simple cycles. Since cycles have constant pathwidth (namely 2), this immediately shows that we cannot expect an FPT (or even an XP) algorithm parameterized by pathwidth alone unless $P = NP$. The same holds for parametrizations with respect to treewidth since the treewidth of a graph is upper bounded by its pathwidth.

In related work, Bannister et al. [6] showed that several problems of compacting *not necessarily planar* orthogonal graph drawings to use the minimum number of rows, area, length of longest edge, or total edge length cannot be approximated better than within a polynomial factor of optimal (if $P \neq NP$). They also provided an FPT algorithm for testing whether a drawing can be compacted to a number of rows k ; the algorithm is parameterized by the natural parameter k . Note that their algorithm does not solve the planar case because the algorithm is allowed to change the embedding.

The research in this paper is motivated by the relevance of the OC problem and by the growing interest in parameterized approaches for NP-hard problems in graph drawing [7]. Recent works on the subject include parameterized algorithms for book embeddings and queue layouts [8, 9, 10, 11, 12], upward planar drawings [11, 13], orthogonal planarity testing and grid recognition [14, 15], clustered planarity and hybrid planarity [16, 17, 18], 1-planar drawings [19], crossing minimization [20, 21, 22], and visual complexity [23, 24, 25].

Contribution. Extending this line of research, we initiate the study of the parameterized complexity of OC and investigate several parameters:

- *Number of kitty corners.* Given that OC can be solved efficiently for orthogonal representations without kitty corners, the number of kitty corners (that is, the number of corners involved in some pair of kitty corners) is a very natural parameter for OC. We show that OC is fixed-parameter tractable (FPT) with respect to the number of kitty corners ([Theorem 1 in Section 3](#)).
- *Number of faces.* Since OC remains NP-hard for orthogonal representations of simple cycles [5], OC is para-NP-hard when parameterized by the number of faces. Hence, we cannot expect an FPT (or even an XP) algorithm in this parameter alone, unless $P = NP$. However, for orthogonal representations of simple cycles we show the existence of a polynomial kernel for OC when parameterized by the number of kitty corners ([Theorem 2 in Section 4](#)).
- *Maximum face-degree.* The maximum face-degree is the maximum number of vertices on the boundary of a face. Since both the NP-hardness reductions by Patrignani [4] and by Evans et al. [5] require faces of linear size, it is interesting to know whether faces of constant size make the problem tractable. We prove that this is not the case, i.e., OC remains NP-hard when parameterized by the maximum face degree ([Theorem 3 in Section 5](#)).
- *Height.* The *height* of an orthogonal representation is the minimum number of distinct y-coordinates required to draw the representation. Since a $w \times h$ grid has pathwidth at most h , graphs with bounded height have bounded pathwidth, but the converse is generally not true [26]. In fact, we show that OC admits an XP algorithm parameterized by the height of the given representation (see [Theorem 4 in Section 6](#)). In this context, we remark that a related problem has been considered by Chaplick et al. [27]. Namely, given a planar graph G , they define $\bar{\pi}_2^1(G)$ to be the minimum number of distinct y-coordinates required to draw the graph straight-line, and provide lower and upper bounds on this parameter. In their setting, however, the embedding of G is not fixed, and the graph is not necessarily drawn in the orthogonal drawing style.

We start with some basics in [Section 2](#) and close with open problems in [Section 7](#).

2. Basic Definitions

Let $G = (V, E)$ be a connected planar graph of vertex-degree at most four and let Γ be a planar orthogonal drawing of G . We assume that in Γ all the vertices and bends have integer coordinates, i.e., we assume that Γ is an integer-coordinate grid drawing. The connected regions of the plane determined by Γ are called *faces*; each face is described by the clockwise sequence of vertices and edges along its boundary. Exactly one of these faces is an infinite region and it is called the *external face* (or *outer face*). The other faces of Γ are the *internal faces*. The *planar embedding* of Γ is the set of (internal and external) faces determined by Γ . Given a face f of Γ , the *degree of f* is the number of vertices traversed while walking clockwise on its boundary, where each vertex is counted the number of times it is traversed (if G is biconnected, each vertex of f is traversed exactly once).

Two planar orthogonal drawings Γ_1 and Γ_2 of G are *shape-equivalent* if: (i) Γ_1 and Γ_2 have the same planar embedding; (ii) for each vertex $v \in V$, the geometric angles at v (formed by any two consecutive edges incident on v) are the same in Γ_1 and Γ_2 ; (iii) for each edge $e = (u, v) \in E$ the sequence of left and right bends along e while moving from u to v is the same in Γ_1 and Γ_2 . An *orthogonal representation* H of G is a class of shape-equivalent planar orthogonal drawings of G . It follows that an orthogonal representation H is completely described by a planar embedding of G , by the values of the angles around each vertex (each angle being a value in the set $\{90^\circ, 180^\circ, 270^\circ, 360^\circ\}$), and by the ordered sequence of left and right bends along each edge (u, v) , moving from u to v ; if we move from v to u , then this sequence and the direction (left/right) of each bend are reversed. If Γ is a planar orthogonal drawing in the class H , then we also say that Γ is a drawing of H . Without loss of generality, we also assume that an orthogonal representation H comes with a given “orientation”, i.e., for each edge segment \overline{pq} of H (where p and q correspond to vertices or bends), we fix whether p lies to the left, to the right, above, or below q .

Turn-regular orthogonal representations. Let H be a planar orthogonal representation. For the purpose of the OC problem, and without loss of generality, we always assume that each bend in H is replaced by a degree-2 vertex, i.e., H is a *rectilinear representation* (each edge is either a horizontal or a vertical segment). Let f be a face of H and assume that the boundary of f is traversed counterclockwise (resp. clockwise) if f is internal (resp. external).

Let u and v be two reflex vertices of f . Let $\text{rot}(u, v)$ be the number of convex corners minus the number of reflex corners encountered while traversing the boundary of f from u (included) to v (excluded); a reflex vertex of degree one is counted like two reflex vertices. We say that u and v is a pair of *kitty corners* of f if $\text{rot}(u, v) = 2$ or $\text{rot}(v, u) = 2$. A vertex is a kitty corner if it is part of a pair of kitty corners. A face f of H is *turn-regular* if it does not contain a pair of kitty corners. The representation H is *turn-regular* if all faces are turn-regular.

Parameterized Complexity. Let Π be an NP-hard problem. In the framework of parameterized complexity, each instance of Π is associated with a *parameter* k . Here, the goal is to confine the combinatorial explosion in the running time of an algorithm for Π to depend only on k . Formally, we say that Π is *fixed-parameter tractable (FPT)* if any instance (I, k) of Π is solvable in time $f(k) \cdot |I|^{O(1)}$, where f is an arbitrary computable function of k . A weaker request is that for every fixed k , the problem Π would be solvable in polynomial time. Formally, we say that Π is *slice-wise polynomial (XP)* if any instance (I, k) of Π is solvable in time $f(k) \cdot |I|^{g(k)}$, where f and g are arbitrary computable functions of k .

A companion notion of fixed-parameter tractability is that of *kernelization*. A *compression algorithm* from a problem Π to a problem Π' is a polynomial-time algorithm that transforms an arbitrary instance of Π to an equivalent instance of Π' whose size is bounded by some computable function g of the parameter k of the original instance. When $\Pi' = \Pi$, then the compression algorithm is called a kernelization algorithm, and the resulting instance is called a *kernel*. Further, we say that Π admits a compression (or a kernel) of size $g(k)$ where k is the parameter. It is well known that a problem is fixed-parameter tractable (FPT) by a parameter k if and only if it admits a kernelization algorithm for the parameter k . If $g(k)$ is the size of a kernel and g is a polynomial function, then the compression (or kernel) is called a *polynomial compression* (or *polynomial kernel*). For more information on parameterized complexity, we refer to books such as [28, 29, 30].

3. Number of Kitty Corners: An FPT Algorithm

Turn-regular orthogonal representations can be compacted optimally in linear time [3]. The result in [3] exploits an interesting relationship between planar orthogonal representations and upward planar embeddings. In the

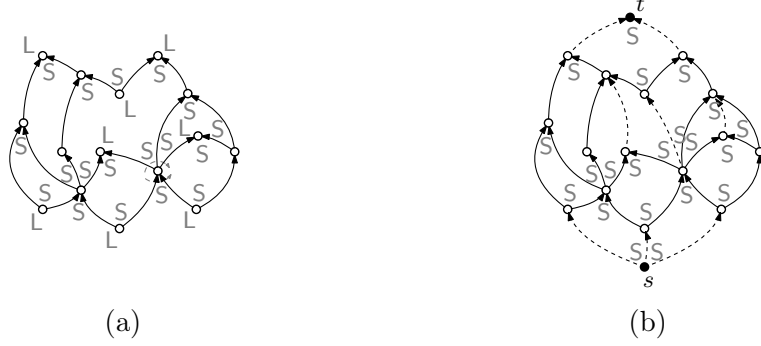


Figure 2: (a) An upward plane DAG D and the corresponding upward labeling. (b) A plane *st*-graph obtained by augmenting D with a complete saturator (dotted edges).

following, we first introduce the necessary terminology about upward planarity, then we recall the result of [3], and finally describe our FPT algorithm.

Upward planar embeddings and saturators. Let $D = (V, E)$ be a plane DAG, i.e., an acyclic digraph with a given planar embedding. An *upward planar drawing* Γ of D is an embedding-preserving drawing of D where each vertex v is mapped to a distinct point of the plane and each edge is drawn as a simple Jordan arc monotonically increasing in the upward direction. Such a drawing exists if and only if D is the spanning subgraph of a plane *st-graph*, i.e., a plane digraph with a unique source s and a unique sink t , which are both on the external face [31]. Let S be the set of sources of D , T be the set of sinks, and $I = V \setminus (S \cup T)$. D is *bimodal* if, for every vertex $v \in I$, the outgoing edges (and hence the incoming edges) of v are consecutive in the clockwise order around v . If an upward planar drawing Γ of D exists, then D is necessarily bimodal and Γ uniquely defines the left-to-right orderings of the outgoing and incoming edges of each vertex. This set of orderings (for all vertices of D) is an *upward planar embedding* of D , and is regarded as an equivalence class of upward planar drawings of D . A plane DAG with a given upward planar embedding is an *upward plane DAG*.

Let e_1 and e_2 be two consecutive edges on the boundary of a face f of a bimodal plane digraph D , and let v be their common vertex. Vertex v is a *source switch of f* (resp. a *sink switch of f*) if both e_1 and e_2 are outgoing edges (resp. incoming edges) of v . Note that, for each face f , the number n_f of source switches of f equals the number of sink switches of f . The

capacity of f is the function $\text{cap}(f) = n_f - 1$ if f is an internal face and $\text{cap}(f) = n_f + 1$ if f is the external face. If Γ is an upward planar drawing of D , then each vertex $v \in S \cup T$ (i.e., a source or a sink) has exactly one angle larger than 180° , called a *large angle*, in one of its incident faces, and $\deg(v) - 1$ angles smaller than 180° , called *small angles*, in its other incident faces. For a source or sink switch of f , assign either a label L or a label S to its angle in f , depending on whether this angle is large or small. For each face f of D , the number of L -labels determined by Γ equals $\text{cap}(f)$ [32]. Conversely, suppose given an assignment of L - and S -labels to the angles at the source and sink switches of D ; for each vertex v , $\mathsf{L}(v)$ (resp. $\mathsf{S}(v)$) denotes the number of L - (resp. of S -) labels at the angles of v . For each face f , $\mathsf{L}(f)$ (resp. $\mathsf{S}(f)$) denotes the number of L - (resp. of S -) labels at the angles in f . Such an assignment corresponds to the labels induced by an upward planar drawing of D if and only if the following properties hold [32]: (a) $\mathsf{L}(v) = 0$ for each $v \in I$ and $\mathsf{L}(v) = 1$ for each $v \in S \cup T$; (b) $\mathsf{L}(f) = \text{cap}(f)$ for each face $f \in F$. We call such an assignment an *upward labeling of D* , as it uniquely corresponds to (and hence describes) an upward planar embedding of D ; see Fig. 2a. We will implicitly assume that a given upward plane DAG is described by an upward labeling.

Given an upward plane DAG D , a *complete saturator* of D is a set of vertices and edges, not belonging to D , used to augment D to a plane st -graph D' . More precisely, a complete saturator consists of a source s and a sink t , which will belong to the external face of D' , and of a set of edges where each edge (u, v) is called a *saturating edge* and fulfills one of the following conditions (see, e.g., Fig. 2b): (i) $u, v \notin \{s, t\}$ and u, v are both source switches of the same face f such that u has label S in f and v has label L in f ; in this case u *saturates* v . (ii) $u, v \notin \{s, t\}$ and u, v are both sink switches of the same face f such that u has label L in f and v has label S in f ; in this case v *saturates* u . (iii) $u = s$ and v is a source switch of the external face with an L angle. (iv) $v = t$ and u is a sink switch of the external face with an L angle.

Compaction of turn-regular representations. We now recall how to compact in linear time a turn-regular rectilinear representation with the approach of [3]. Consider first any planar rectilinear representation H , which is not necessarily turn-regular. Let D_x be the plane DAG whose vertices correspond to the maximal vertical chains of H and such that two vertices of D_x are connected by an edge oriented rightward, if the corresponding vertical chains are connected by a horizontal segment in H . Define the upward plane DAG

D_y symmetrically, where the vertices correspond to the maximal horizontal chains of H and where the edges are oriented upward. Refer to Fig. 3. D_x and D_y are both upward plane DAGs (for D_x rotate it by 90° to see all edges flowing in the upward direction). For a vertex v of H , $c_x(v)$ (resp. $c_y(v)$) denotes the vertex of D_x (resp. of D_y) corresponding to the maximal vertical (resp. horizontal) chain of H that contains v . For any two vertices u and v of H such that $c_x(u) \neq c_x(v)$, we write $u \rightsquigarrow_x v$ if there exists a directed path from $c_x(u)$ to $c_x(v)$ in D_x . We also write $u \rightsquigleftarrow_x v$ if either $u \rightsquigarrow_x v$ or $v \rightsquigarrow_x u$, while $u \not\rightsquigarrow_x v$ means that neither $u \rightsquigarrow_x v$ nor $v \rightsquigarrow_x u$. The notations $u \rightsquigarrow_y v$, $v \rightsquigarrow_y u$, $u \rightsquigleftarrow_y v$, and $u \not\rightsquigarrow_y v$ are used symmetrically referring to D_y when $c_y(u) \neq c_y(v)$.

Bridgeman et al. [3] showed that H is turn-regular if and only if, for every two vertices u and v in H , we have $u \rightsquigleftarrow_x v$, or $u \rightsquigleftarrow_y v$, or both. This is equivalent to saying that the relative position along the x -axis or the relative position along the y -axis (or both) between u and v is fixed over all drawings of H . Under this condition, the OC problem for H can be solved by independently solving in $O(n)$ time a pair of 1D compaction problems for H , one in the x -direction and the other in the y -direction. The 1D compaction in the x -direction consists of: (i) augmenting D_x to become a plane st -graph by means of a complete saturator; (ii) computing an optimal topological numbering X of D_x (see [1], p. 89); each vertex v of H receives an x -coordinate $x(v)$ such that $x(v) = X(c_x(v))$. We recall that a topological numbering of a DAG D is an assignment of integer numbers to the vertices of D such that if there is a path from u to v then u is assigned a number smaller than the number of v . A topological numbering is optimal if the range of numbers that is used is the minimum possible. Regarding step (i) of the 1D compaction, note that D_x admits a unique complete saturator when H is turn-regular [3]. This is due to the absence of kitty corners in each face of H . The 1D compaction in the y -direction is solved symmetrically, so that each vertex v receives a y -coordinate $y(v) = Y(c_y(v))$. Figure 3 illustrates this process.

Unfortunately, if H is not turn-regular, the aforementioned approach fails. This is because there are in general many potential complete saturators for augmenting the two upward plane DAGs D_x and D_y to plane st -graphs. Also, even when an st -graph for each DAG is obtained from a complete saturator, computing independently an optimal topological numbering for each of the two st -graphs may lead to non-planar drawings if no additional relationships are established for the coordinates of kitty corner pairs, because for a pair

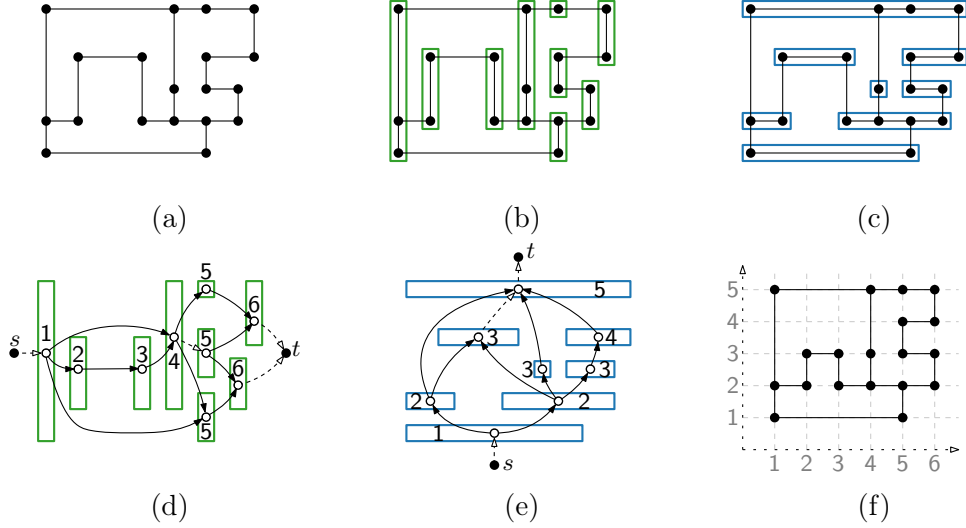


Figure 3: (a) A turn-regular orthogonal representation H . (b)–(c) The maximal horizontal and vertical chains of H are highlighted. (d) The upward plane DAG D_x with its complete saturator (dashed edges) and an optimal topological numbering. (e) The same for D_y . (f) A minimum-area drawing of H where the x- and y-coordinates correspond to the two optimal topological numberings.

$\{u, v\}$ of kitty corners we have $u \not\sim_x v$ and $u \not\sim_y v$.

Our FPT algorithm. We now prove that OC is fixed-parameter-tractable when parameterized by the number of kitty corners.

Theorem 1. *Given a planar rectilinear representation H with n vertices and $k > 0$ kitty corners, we can compute a minimum-area drawing of H in $O(2^{8.4k}n \log n)$ time. In other words, OC is FPT when parameterized by k .*

Proof. For each pair $\{u, v\}$ of kitty corners in each face, we guess the relative positions of u and v in a drawing of H , i.e., $x(u) \leq x(v)$ and $y(u) \leq y(v)$. This implies $O(k^2)$ guesses.

More precisely, we generate all maximal plane DAGs (together with an upward planar embedding) that can be incrementally obtained from D_x by repeatedly applying the following sequence of steps: Guess a pair $\{u, v\}$ of kitty corners of H such that $c_x(u)$ and $c_x(v)$ belong to the same face; for such a pair either add a directed edge $(c_x(u), c_x(v))$ (which establishes that $x(u) < x(v)$), or add a directed edge $(c_x(v), c_x(u))$ (which establishes that

$x(u) > x(v)$), or identify $c_x(u)$ and $c_x(v)$ (which establishes that $x(u) = x(v)$); this last operation corresponds to adding in H a vertical segment between u and v , thus merging the vertical chain of u with the vertical chain of v . Analogously, we generate from D_y a set of maximal plane DAGs (together with an upward planar embedding). Let $\overline{D_x}$ and $\overline{D_y}$ be two upward plane DAGs generated from D_x and D_y , respectively, as described above. We augment $\overline{D_x}$ (resp. $\overline{D_y}$) with a complete saturator that makes it a plane st -graph. Observe that, by construction, neither $\overline{D_x}$ nor $\overline{D_y}$ contain two non-adjacent vertices in the same face whose corresponding chains of H have a pair of kitty corners. Hence their complete saturators are uniquely defined. We finally compute a pair of optimal topological numberings to determine the x - and the y -coordinates of each vertex of H using the algorithm of Bridgeman et al. [3]. Note that, for some pairs of $\overline{D_x}$ and $\overline{D_y}$, the procedure described above may assign x - and y -coordinates to the vertices of H that do not lead to a planar orthogonal drawing. If so, we discard the solution. Conversely, for those solutions that correspond to (planar) drawings of H , we compute the area and, at the end, we keep one of the drawings having minimum area.

Figure 4 shows an example of a non-turn-regular orthogonal representation; Fig. 4d depicts four distinct drawings resulting from different pairs of upward plane DAGs, each establishing different x - and y -relationships between pairs of kitty corners. One of the drawings has minimum area; another one is not planar and therefore discarded.

We now analyze the time complexity of the given algorithm. Let $\{f_1, f_2, \dots, f_h\}$ be the set of faces of H , and let k_i be the number of kitty corners in f_i (i.e., the number of vertices that are involved in at least one pair of kitty corners). Since kitty corners are reflex, a vertex can be a kitty corner at most with respect to one face. Hence, $\sum_{i=1}^h k_i = k$.

Denote by a_i the number of distinct maximal planar augmentations of f_i with edges that connect pairs of kitty corners. An upper bound to the value of a_i is the number c_{k_i} of distinct maximal outerplanar graphs with k_i vertices, which corresponds to the number of distinct triangulations of a convex polygon with k_i vertices. It is known that c_{k_i} equals the $(k_i - 2)$ -nd Catalan number (see, e.g., [33]), whose standard estimate is $c_{k_i-2} \sim \frac{4^{k_i-2}}{(k_i-2)^{3/2}\sqrt{\pi}}$. Therefore, $a_i \leq 4^{k_i}$. Note that, from an algorithmic point of view, all distinct triangulations of a convex polygon with given set of vertices can easily be generated with a recursive approach: every time we guess an edge, it divides an internal face into two faces, and in each of the two faces we recursively

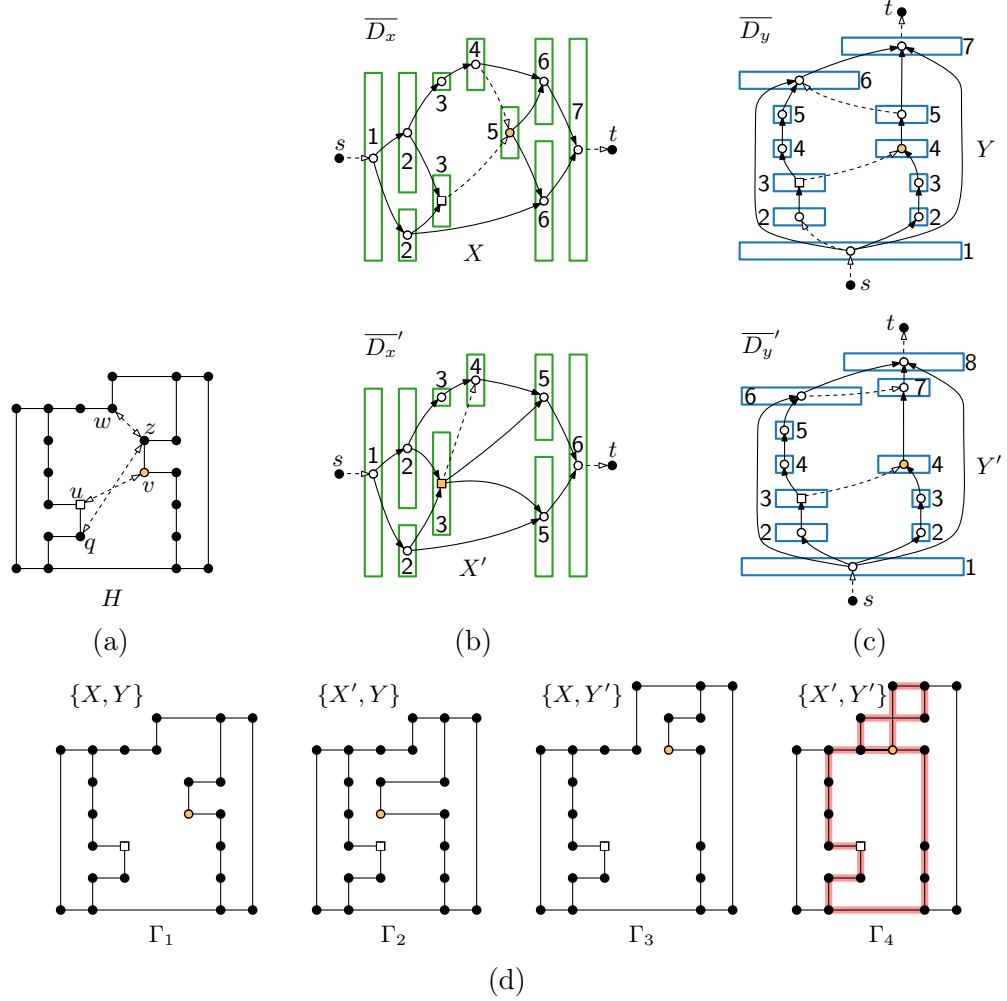


Figure 4: (a) An orthogonal representation H with three pairs of kitty corners, $\{u, v\}$, $\{w, z\}$, $\{q, z\}$, and $k = 5$ kitty corners in total. (b) Two distinct (saturated) upward plane DAGs \overline{D}_x and \overline{D}'_x , and their optimal topological numberings X and X' ; in \overline{D}'_x the nodes $c_x(u)$ and $c_x(v)$ are identified (filled square). (c) Two distinct (saturated) upward plane DAGs \overline{D}_y and \overline{D}'_y , and their optimal topological numberings Y and Y' . (d) Drawings derived from the four different combinations of the topological numberings: Γ_1 and Γ_3 have sub-optimal areas, Γ_2 has minimum area, and Γ_4 is non-planar (the bold red face is self-crossing).

guess the next edge.

Now, for each edge (u, v) of a maximal planar augmentation of f_i such that $\{u, v\}$ is a pair of kitty corners in H , we have to consider three alternative possibilities: $\overline{D_x}$ has a directed edge $(c_x(u), c_x(v))$, or $\overline{D_x}$ has a directed edge $(c_x(v), c_x(u))$, or $c_x(u)$ and $c_x(v)$ are identified in $\overline{D_x}$.

Recall that the number of edges of a maximal outerplanar graph on k_i vertices is $2k_i - 3$. Hence, for each augmentation of H that adds m_i edges inside each face f_i , we have $m_i \leq 2k_i - 3$, i.e., H consists of $\sum_{i=1}^h m_i \leq \sum_{i=1}^h (2k_i - 3) \leq 2k$ edges. Therefore, the number of different possibilities to be considered for $\overline{D_x}$ is at most 3^{2k} . The same holds for $\overline{D_y}$. We have to consider at most $a_i \leq 4^{k_i}$ augmentations for face f_i and at most $\prod_{i=1}^h 4^{k_i} \leq 4^k$ augmentations for the whole graph H .

The total number of augmentation of H times the number of possibilities to extend D_x to $\overline{D_x}$ times the number of possibilities to extend D_y to $\overline{D_y}$ is then $4^k \cdot 3^{2k} \cdot 3^{2k} = 324^k < 2^{8.4k}$. For each of these combinations, we augment the two upward plane DAGs $\overline{D_x}$ and $\overline{D_y}$ to plane st -graphs using complete saturators and compute an optimal topological numbering in $O(n)$ time. Then we test whether the drawing resulting from the two topological numberings is planar, which can be done in $O(n \log n)$ time by a sweep-line algorithm (see, e.g., [34, 35]). It follows that the whole testing algorithm takes $O(2^{8.4k} n \log n)$ time. \square

4. A Polynomial Kernel for Cycle Graphs

In this section, we give a polynomial kernel for cycle graphs parameterized by the number of kitty corners. To this end, without loss of generality, in this section, we consider OC as a decision problem as follows: Given a planar rectilinear representation H of a connected planar graph G and a rectangle \mathcal{B} , decide whether there exists an orthogonal drawing of H having bounding box \mathcal{B} . We prove the following theorem.

Theorem 2. *Parameterized by the number of kitty corners, OC admits a polynomial kernel on cycle graphs.*

Let $[a, b]$ denote the set of natural numbers $\{a, a+1, \dots, b-1, b\}$. We first design a compression with a linear number of vertices for the OC problem on cycle graphs, parameterized by the number of kitty corners. We give a compression algorithm from the OC problem on cycle graphs to the OC problem on cycle graphs with additional weight constraints on edges. We

call this problem the *weighted orthogonal compaction* problem and define it formally as follows. Given a planar rectilinear representation H of a connected planar graph G with integer edge weights and a rectangle \mathcal{B} on the integer grid and of polynomial size, the weighted orthogonal compaction problem (WEIGHTED OC for short) asks whether there exists a drawing of H having bounding box \mathcal{B} such that the length of each edge in the drawing is at least the weight of the edge. At the end of our compression algorithm, by using [Proposition 1](#), we will show how this gives us a polynomial kernel for OC.

Our compression algorithm is presented as a number of reduction rules. A reduction rule is a polynomial-time procedure that replaces an instance (I, k) of a parameterized decision problem Π by a new instance (I', k') of another parameterized decision problem Π' where $|I'| \leq |I|$ and $k' \leq k$. The rule is called *safe* if (I, k) is a *yes* instance of Π if and only if (I', k') is a *yes* instance of Π' .

Let G be a cycle graph and let H be a rectilinear representation of G . As G is a cycle graph, H has only one internal face, f_{int} , which traverses all the vertices and edges of G . Therefore, for ease of writing in this section, whenever we talk about a face of H , we refer to the face f_{int} unless stated otherwise. We traverse the face f_{int} in the counterclockwise direction and define a new labeled directed graph G^\rightarrow as follows. We direct every edge $e = (u, v)$ from u to v such that u comes before v while traversing e . We label every edge as E, W, N, or S depending on whether the edge is directed in the east, west, north, or south direction, respectively. Moreover, we label every vertex as F, R, or C if and only if the vertex is a flat, reflex, or convex vertex, respectively. See [Fig. 5](#). For a vertex v , let $\text{label}(v)$ be the label of v in G^\rightarrow . We say that v is a $\text{label}(v)$ -vertex. Similarly, for an edge e , let $\text{label}(e)$ be the label of e in G^\rightarrow . We say that e is a $\text{label}(e)$ -edge. For any two vertices u and v , let $P_{u,v}$ be the directed path from u to v in G^\rightarrow . In the rest of this section, we talk about the graph G^\rightarrow , unless stated otherwise. Moreover, when we talk about a drawing Γ of G^\rightarrow , we refer to a planar (orthogonal) drawing of H . Furthermore, when we talk about a labeling of a path of G^\rightarrow , we talk about vertex labeling, unless stated otherwise.

As every vertex v in G has degree 2, v has exactly one incoming edge and one outgoing edge in G^\rightarrow . Let $\text{prev}(v)$ and $\text{next}(v)$ be the incoming edge to v and the outgoing edge from v , respectively. We call the ordered pair $(\text{label}(\text{prev}(v)), \text{label}(\text{next}(v)))$ the *edge label pair associated* to v . Observe that v is an F-vertex if and only if its associated edge label pair belongs to the set $\{(E, E), (W, W), (N, N), (S, S)\}$. Similarly, v is an R-vertex (resp.,

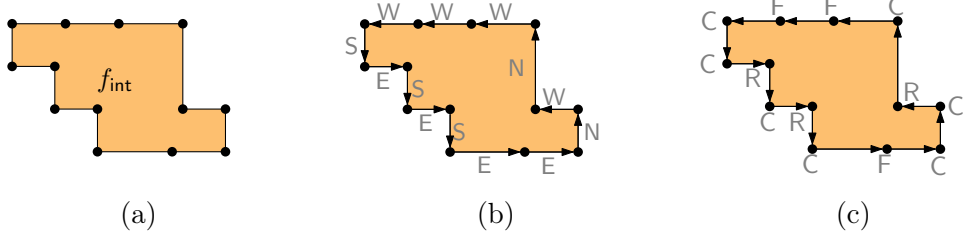


Figure 5: An illustration of (a) a cycle graph G and the corresponding (b) labeled directed edges and (c) labeled vertices of G^\rightarrow .

a C -vertex) if and only if its associated edge label pair belongs to the set $\{(W, N), (N, E), (E, S), (S, W)\}$ (resp., $\{(W, S), (S, E), (E, N), (N, W)\}$).

We denote by (v, E) , (v, W) , (v, N) and (v, S) the ray with the endpoint v and going in the east, west, north and south direction, respectively. Let each of ℓ_1 and ℓ_2 be a ray or a line segment. We denote by $\text{intPoint}(\ell_1, \ell_2)$ the intersection point of ℓ_1 and ℓ_2 (if it exists). Given an edge e , we denote by $\text{weight}(e)$ the weight of the edge e . We initialize all edge weights to be 1.

Let $\langle c_1, c_2, \dots, c_k, c_{k+1} = c_1 \rangle$ be the cyclic counterclockwise order of kitty corners of H in G^\rightarrow . We look at the path $P_{c_i, c_{i+1}}$, for every $i \in [1, k]$, and bound the number of internal vertices of this path as a function of k . As G^\rightarrow is the union of all such paths, this, in turn, will bound the size of the reduced instance as a function of k . We will give a series of reduction rules to reduce the number of vertices of such paths. We will always apply the rules in the order they are given. This, in turn, implies that when we apply some Reduction Rule i on an instance, no other Reduction Rule j with $j < i$ can be further applied to the instance.

We start with a simple reduction rule that reduces a path P on F -vertices to a weighted edge. Formally, we have the following rule.

Reduction Rule 1. *Suppose that there exists a path $P = (u_1, u_2, \dots, u_t)$ in G^\rightarrow such that $t \geq 3$ and $\text{label}(u_i) = F$ for every $i \in [2, k - 1]$. Then, delete the path (u_2, \dots, u_{t-1}) and connect u_1 to u_t by a directed edge from u_1 to u_t whose weight is the sum of the weights of the edges of P .*

This reduction rule is safe because a path on F -vertices is always drawn as a straight line path between its end points in any drawing of G^\rightarrow such that the length of the path is at least its weight. So we can replace the path with a straight-line edge between its end points whose weight is the sum of the weights of the edges of the path, and vice-versa.

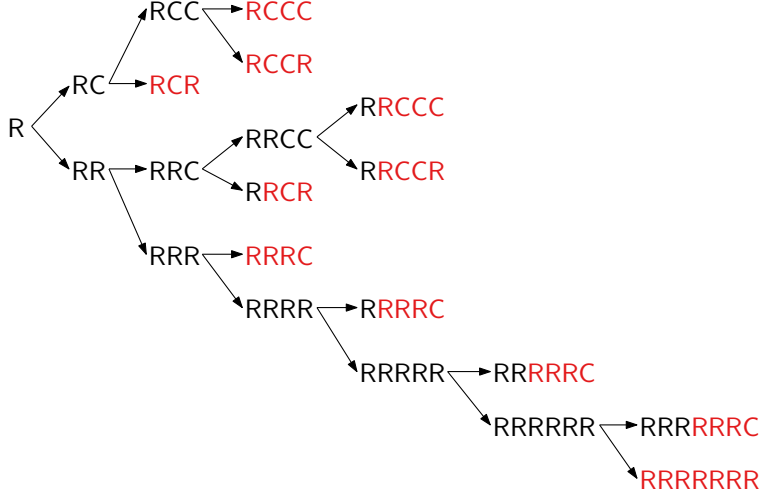


Figure 6: An illustration showing that a path on 7 or more vertices starting with an R-vertex has either only R-vertices or a subpath (shown in red) whose labeling belongs to the set $\{RCR, RCCC, RCCR, RRRC\}$. The case of a path starting with a C-vertex is symmetric and thus not shown in the figure.

As we apply the reduction rules in order, due to [Reduction Rule 1](#), for the rest of the section, we assume that G^\rightarrow does not have any F-vertex. So, all the internal vertices of $P_{c_i, c_{i+1}}$, for any $i \in [1, k]$, are R- or C-vertices and none of them are kitty corners of H . Let $P_{c_i, c_{i+1}} = (v_1 = c_i, v_2, \dots, v_t = c_{i+1})$. If $t \leq 16$, we do not reduce the path $P_{c_i, c_{i+1}}$. Otherwise, we reduce the truncated path $P_{c_i, c_{i+1}}^{\text{trun}} = (v_6, v_7, \dots, v_{t-5})$, leaving five buffer vertices on both the sides. These buffer vertices will be helpful later in our reduction rules. Note that the number of vertices of $P_{c_i, c_{i+1}}^{\text{trun}}$ is at least 7 for any $i \in [1, k]$. We now give the following observation about $P_{c_i, c_{i+1}}^{\text{trun}}$, which will be useful in designing our reduction rules.

Observation 1. *Let $i \in [1, k]$. The path $P_{c_i, c_{i+1}}^{\text{trun}}$ has either only R-vertices or a subpath whose labeling belongs to the set $\{RCR, RCCC, RCCR, RRRC, CRC, CRRC, CRRC, CCCR\}$. See [Fig. 6](#).*

Due to the above observation, we only give reduction rules for the (sub)paths whose labeling belongs to the set $\{RCR, RCCC, RCCR, RRRC, CRC, CRRC, CRRC, CCCR\}$. Before we start with our reduction rules, given an R- or a C-vertex v and a drawing Γ of G^\rightarrow , we define two vertices $\text{nearX}(v, \Gamma)$ and $\text{nearY}(v, \Gamma)$, called the *nearest y-vertex* and the *nearest x-vertex* of v in

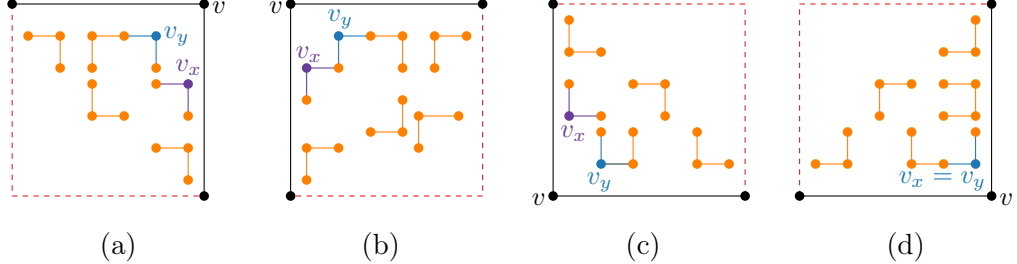


Figure 7: An illustration for the definitions of $\text{nearX}(v, \Gamma)$ (shown by v_x) and $\text{nearY}(v, \Gamma)$ (shown by v_y). The corresponding definitions are given in Observations 2, 4, 5 and 6 are illustrated in (a), (b), (c) and (d), respectively.

Γ , respectively. Note that $\text{nearX}(v, \Gamma)$ can be the same as $\text{nearY}(v, \Gamma)$. Intuitively, $\text{nearX}(v, \Gamma)$ (resp., $\text{nearY}(v, \Gamma)$) is the vertex of G^\rightarrow in the minimum size rectangle bounding v , $\text{prev}(v)$ and $\text{next}(v)$, which is “nearest” to v in the x-direction (resp., y-direction) and $\text{label}(\text{nearX}(v, \Gamma)) \in \{\text{R}, \text{C}\} \setminus \{\text{label}(v)\}$ (resp., $\text{label}(\text{nearY}(v, \Gamma)) \in \{\text{R}, \text{C}\} \setminus \{\text{label}(v)\}$) (see Fig. 7).

Although the total number of different edge label pair associated with an R- or a C-vertex is 8, for defining the above two vertices we need to look at only 4 pairs of edge label pairs corresponding to either an R- or a C-vertex as the other 4 are symmetric in the following sense. If we describe the neighbors of a vertex v as to the right of v and above v , then v is either an R-vertex with associated edge label pair (W, N) or a C-vertex with associated edge label pair (S, E). Similarly, (N, E), (E, S) and (S, W) are symmetric to (W, S), (N, W) and (E, N), respectively. So, given a C- or R-vertex v , let $\text{left}(v)$, $\text{right}(v)$, $\text{above}(v)$, $\text{below}(v)$ be the vertex which is to the left, to the right, above and below v , if it exists. Observe that given a C- or R-vertex v exactly two out of $\text{left}(v)$, $\text{right}(v)$, $\text{above}(v)$, $\text{below}(v)$ exist. In what follows, we give observations about the existence of $\text{nearX}(v, \Gamma)$ and $\text{nearY}(v, \Gamma)$ and some of their properties (see Fig. 7).

Observation 2. Let v be an R- or a C-vertex of G^\rightarrow such that $\text{left}(v)$ and $\text{below}(v)$ exist. Let Γ be a drawing of G^\rightarrow such that there exists a vertex u for which (i) $x(u) \in [x(\text{left}(v)), x(\text{below}(v))]$, (ii) $y(u) \in [y(\text{below}(v)), y(\text{left}(v))]$, and (iii) $u, \text{prev}(u), \text{next}(u) \notin \{\text{left}(v), \text{below}(v)\}$. Let S be the set of all such vertices. Let $\text{maxY} = \max\{y(v) \mid v \in S\}$ and $\text{maxX} = \max\{x(v) \mid v \in S\}$.

Then, $\text{nearX}(v, \Gamma)$ is the vertex in S such that $x(\text{nearX}(v, \Gamma)) = \text{maxX}$ and $y(\text{nearX}(v, \Gamma)) = \max\{y(v) \mid v \in S \wedge x(v) = \text{maxX}\}$. Similarly, $\text{nearY}(v, \Gamma)$

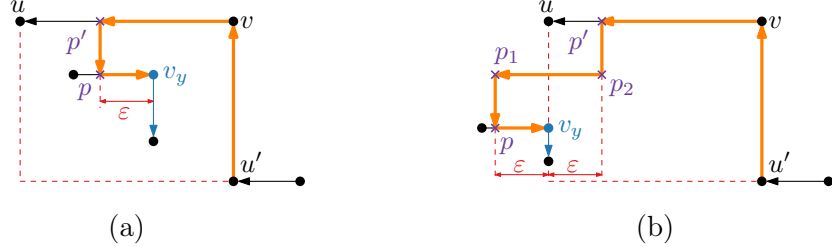


Figure 8: Illustration for the two cases considered in the proof of Lemma 1 based on the relative positions of $\text{next}(v)$ (shown by u) and $\text{nearY}(v, \Gamma)$ (shown by v_y). (a) The case where $x(\text{nearY}(v, \Gamma)) > x(\text{next}(v))$. (b) The case where $x(\text{nearY}(v, \Gamma)) = x(\text{next}(v))$. The paths from $\text{prev}(v)$ (shown by u') to $\text{nearY}(v, \Gamma)$, to show that they are a pair of kitty corners, are drawn in orange.

is the vertex in S such that $y(\text{nearY}(v, \Gamma)) = \text{maxY}$ and $x(\text{nearY}(v, \Gamma)) = \text{max}\{x(v) \mid v \in S \wedge y(v) = \text{maxY}\}$. It follows from the definition that the neighbors of $\text{nearX}(v, \Gamma)$ (resp., $\text{nearY}(v, \Gamma)$) are to the left of and below $\text{nearX}(v, \Gamma)$ (resp., $\text{nearY}(v, \Gamma)$). Moreover, from the planarity of Γ , it follows that $\text{label}(\text{nearX}(v, \Gamma)) \in \{\text{R}, \text{C}\} \setminus \{\text{label}(v)\}$ and $\text{label}(\text{nearY}(v, \Gamma)) \in \{\text{R}, \text{C}\} \setminus \{\text{label}(v)\}$. See Fig. 7a.

As the observation for the remaining cases, i.e. when either $\text{right}(v)$ and $\text{below}(v)$ (Fig. 7b), or $\text{right}(v)$ and $\text{above}(v)$ (Fig. 7c), or $\text{left}(v)$ and $\text{above}(v)$ (Fig. 7d) exist, are similar to Observation 2, they are given as Observations 4–6 in the Appendix. For ease of writing, if drawing is clear from the context, we may refer $\text{nearX}(v, \Gamma)$ and $\text{nearY}(v, \Gamma)$ as $\text{nearX}(v)$ and $\text{nearY}(v)$, respectively.

Let v be an R- or a C-vertex of G^\rightarrow . Based on these observations, we now give a lemma about the existence of kitty corner pairs (c, c') , where $c \in \{\text{prev}(v), \text{next}(v)\}$ and $c' \in \{\text{nearX}(v, \Gamma), \text{nearY}(v, \Gamma)\}$.

Lemma 1. *Let v be an R- or a C-vertex of G^\rightarrow . Let Γ be a drawing of G^\rightarrow such that $\text{nearX}(v, \Gamma)$ and $\text{nearY}(v, \Gamma)$ exist. If $\text{label}(\text{prev}(v)) = \text{label}(\text{nearX}(v, \Gamma))$ (resp., $\text{label}(\text{next}(v)) = \text{label}(\text{nearX}(v, \Gamma))$), then $(\text{prev}(v), \text{nearX}(v, \Gamma))$ and $(\text{prev}(v), \text{nearY}(v, \Gamma))$ (resp., $(\text{next}(v), \text{nearX}(v, \Gamma))$ and $(\text{next}(v), \text{nearY}(v, \Gamma))$) are kitty corners of H .*

Proof. We prove the lemma for $\text{prev}(v)$ and $\text{nearY}(v, \Gamma)$ for a C-vertex v . The proofs for the other cases are similar. Without loss of generality, we assume that the edge label pair associated with v is (N, W) . This, in turn, implies

that $\text{label}(\text{prev}(v)) = \text{label}(\text{nearY}(v, \Gamma)) = R$ and the edge label pair associated with $\text{nearY}(v, \Gamma)$ is (E, S) . Moreover, there also exists a path from $\text{nearY}(v, \Gamma)$ to v . We consider two cases based on whether $x(\text{nearY}(v, \Gamma)) = x(\text{next}(v))$ or $x(\text{nearY}(v, \Gamma)) > x(\text{next}(v))$.

Let $\varepsilon \in \mathbb{R}$ such that $0 < \varepsilon < 1$. Let p be a point that is immediately to the left of $\text{nearY}(v, \Gamma)$ on the line segment corresponding to the edge $(\text{prev}(\text{nearY}(v, \Gamma)), \text{nearY}(v, \Gamma))$ in Γ , such that $x(p) = x(\text{nearY}(v, \Gamma)) - \varepsilon$. We first consider the case where $x(\text{nearY}(v, \Gamma)) > x(\text{next}(v))$ (see Fig. 8a). Let p' be the point on the line segment corresponding to the edge $(v, \text{next}(v))$ in Γ such that $x(p') = x(p)$. From the definitions of $\text{nearY}(v, \Gamma)$, p and p' , we have that the line segment (p, p') does not intersect any line segment in Γ . We now focus on the directed cycle graph \mathcal{C} formed by the path from $\text{nearY}(v, \Gamma)$ to v in G^\rightarrow followed by the path $(v, p', p, \text{nearY}(v, \Gamma))$ where $\text{label}(p) = \text{label}(p') = C$, $\text{label}((v, p')) = W$, $\text{label}((p', p)) = S$, $\text{label}((p, \text{nearY}(v, \Gamma)) = E$ and the labels of all the other vertices and edges remain as in G^\rightarrow . Observe that by the construction, there exists a planar drawing of \mathcal{C} . As $\text{rot}(\text{prev}(v), \text{nearY}(v, \Gamma)) = (-1) + 1 + 1 + 1 = 2$, $\text{rot}(\text{nearY}(v, \Gamma), \text{prev}(v)) = 2$. As the path from $\text{nearY}(v, \Gamma)$ to $\text{prev}(v)$ in \mathcal{C} is the same as that in G^\rightarrow , $(\text{nearY}(v, \Gamma), \text{prev}(v))$ is a pair of kitty corners of H .

We now consider the case where $x(\text{nearY}(v, \Gamma)) = x(\text{next}(v))$ (see Fig. 8b). Let p_1 be a point such that $x(p_1) = x(p)$ and $y(p_1) = y(p) + \varepsilon$. Let p_2 be a point such that $x(p_2) = x(\text{nearY}(v, \Gamma)) + \varepsilon$ and $y(p_2) = y(p_1)$. Let p' be the point on the line segment corresponding to the edge $(v, \text{next}(v))$ in Γ such that $x(p') = x(p_2)$. From the definitions of $\text{nearY}(v, \Gamma)$, p , p_1 , p_2 and p' , we have that the line segments (p, p_1) , (p_1, p_2) and (p_2, p') do not intersect any line segment in Γ . We now focus on the directed cycle graph \mathcal{C} formed by the path from $\text{nearY}(v, \Gamma)$ to v in G^\rightarrow followed by the path $(v, p', p_2, p_1, p, \text{nearY}(v, \Gamma))$ where $\text{label}(p) = \text{label}(p_1) = \text{label}(p') = C$, $\text{label}(p_2) = R$, $\text{label}((v, p')) = W$, $\text{label}((p', p_2)) = S$, $\text{label}((p_2, p_1)) = W$, $\text{label}((p_1, p)) = S$, $\text{label}((p, \text{nearY}(v, \Gamma)) = E$, and the labels of all the other vertices and edges remain as in G^\rightarrow . Observe that by the construction, there exists a planar drawing of \mathcal{C} . As $\text{rot}(\text{prev}(v), \text{nearY}(v, \Gamma)) = (-1) + 1 + 1 + (-1) + 1 + 1 = 2$, $\text{rot}(\text{nearY}(v, \Gamma), \text{prev}(v)) = 2$. As the path from $\text{nearY}(v, \Gamma)$ to $\text{prev}(v)$ in \mathcal{C} is the same as that in G^\rightarrow , $(\text{nearY}(v, \Gamma), \text{prev}(v))$ is a pair of kitty corners of H . \square

Without loss of generality, in the rest of the section, we assume that the first edge of the path we want to reduce is a W -edge. We remark that a

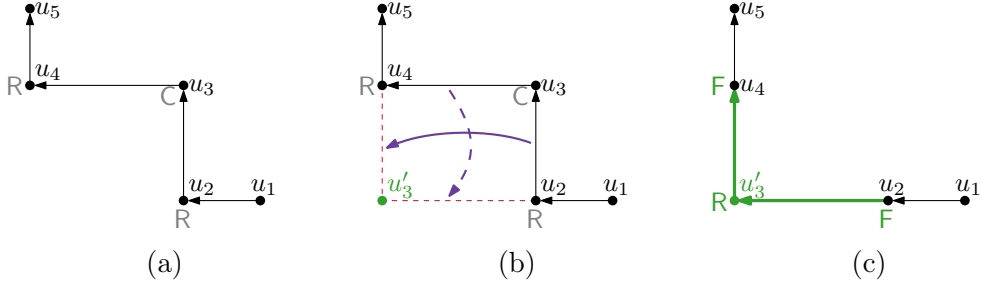


Figure 9: An illustration for Reduction Rule 2. The original path P is shown in (a) and the reduced path is shown in (c). (b) shows the vertex u'_3 , and the projection from the edges of $G^>$ that will be deleted when applying the reduction rule to the edges of $G_{\text{red}}^>$. The projection is shown by curved purple solid and dotted edges from an edge to be deleted to its projected edge.

strategy based on “rectangle cutting” that somewhat resembles our reduction rules has been employed by Tamassia [36] for a different purpose. We now give our reduction rules for a path labeled RCR or CRC. We give the reduction rule for RCR. As the reduction rule for CRC is similar, it is given as Reduction Rule 5 in the Appendix.

Reduction Rule 2. *Suppose that there exists a path $P = (u_1, u_2, u_3, u_4, u_5)$ in $G^>$ such that $\text{label}(u_2) = R$, $\text{label}(u_3) = C$ and $\text{label}(u_4) = R$. Then, delete the vertex u_3 and the edges incident to it from $G^>$ and add a new path (u_2, u'_3, u_4) to $G^>$. Moreover, assign $\text{label}(u_2) = F$, $\text{label}(u'_3) = R$, $\text{label}(u_4) = F$, $\text{weight}((u_2, u'_3)) = \text{weight}((u_3, u_4))$ and $\text{weight}((u'_3, u_4)) = \text{weight}((u_2, u_3))$. The labels of all the remaining vertices and the weights of all the remaining edges stay the same. Let $G_{\text{red}}^>$ be the reduced graph. See Fig. 9.*

Lemma 2. *Reduction Rule 2 is safe.*

Proof. To prove that Reduction Rule 2 is safe, we need to prove that there exists a planar drawing Γ of $G^>$ if and only if there exists a planar drawing Γ_{red} of $G_{\text{red}}^>$ such that both Γ and Γ_{red} have the same bounding box. Recall that, without loss of generality, we assume that $\text{label}((u_1, u_2)) = W$.

(\Rightarrow) Let Γ be a planar drawing of $G^>$ having bounding box \mathcal{B} . We get a drawing Γ_{red} of $G_{\text{red}}^>$ having the same bounding box \mathcal{B} as follows. For every vertex $v \in V(G_{\text{red}}^>) \setminus \{u'_3\}$, $x(v)$ and $y(v)$ in Γ_{red} are the same as those in Γ . For

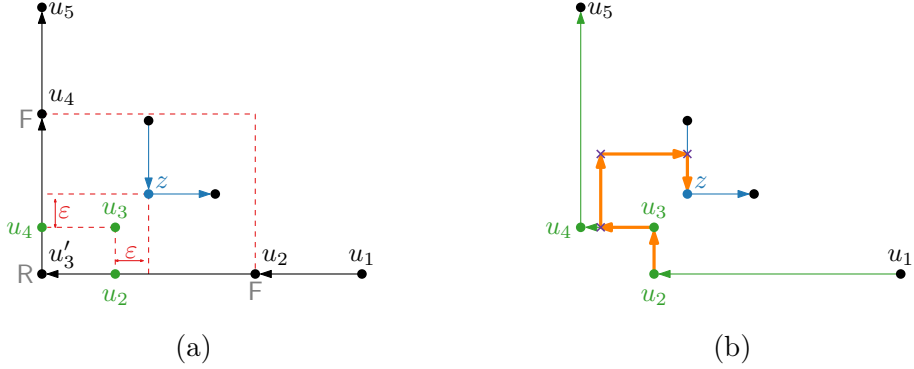


Figure 10: An illustration for the case considered in the reverse direction proof of Lemma 2. A path from u_2 to $\text{nearY}(u'_3, \Gamma)$ (shown by z), to show that they are a pair of kitty corners, are drawn in orange.

u'_3 , we assign $x(u'_3) = x(u_4)$ and $y(u'_3) = y(u_2)$. Observe that \mathcal{B} is a bounding box of Γ_{red} . Moreover, if there does not exist any vertex $w \in V(G^\rightarrow)$ such that $x(w) \in [x(u_4), x(u_2)]$ and $y(w) \in [y(u_2), y(u_4)]$ in Γ , then Γ_{red} is a planar drawing of $G_{\text{red}}^\rightarrow$. Assume for contradiction there exists such a w . Observe that $\text{prev}(w), \text{next}(w) \notin \{u_2, u_4\}$. Then, by Observation 2 and Lemma 1, $\text{nearY}(u_3)$ exists and $(\text{nearY}(u_3), u_2)$ is a kitty corner pair of H , a contradiction to the fact that the path that we are reducing does not contain any kitty corner (as it is a path between two consecutive kitty corner vertices).

(\Leftarrow) Let Γ_{red} be a planar drawing of $G_{\text{red}}^\rightarrow$ having bounding box \mathcal{B} . We get a drawing Γ of G^\rightarrow having the same bounding box \mathcal{B} as follows. For every vertex $v \in V(G^\rightarrow) \setminus \{u_3\}$, $x(v)$ and $y(v)$ in Γ are the same as those in Γ_{red} . For u_3 , we assign $x(u_3) = x(u_2)$ and $y(u_3) = y(u_4)$. Observe that \mathcal{B} is a bounding box of Γ . Moreover, if there does not exist any vertex $w \in V(G_{\text{red}}^\rightarrow)$ such that $x(w) \in [x(u_4), x(u_2)]$ and $y(w) \in [y(u_2), y(u_4)]$ in Γ_{red} , then Γ is a planar drawing of G^\rightarrow . Assume for contradiction there exists such a w . Observe that $\text{prev}(w), \text{next}(w) \notin \{u_2, u_4\}$. Then, by Observation 5, $\text{nearY}(u'_3)$ exists and $\text{label}(\text{nearY}(u'_3)) = \mathcal{C}$. Let Γ' be a drawing of G^\rightarrow obtained from Γ_{red} as follows. Let $\varepsilon \in \mathbb{R}$ such that $0 < \varepsilon < 1$. For every vertex $v \in V(G^\rightarrow) \setminus \{u_2, u_3, u_4\}$, $x(v)$ and $y(v)$ in Γ' are the same as those in Γ_{red} . For u_2 , we assign $x(u_2) = x(\text{nearY}(u'_3)) - \varepsilon$ and $y(u_2) = y(u'_3)$. For u_4 , we assign $x(u_4) = x(u'_3)$ and $y(u_4) = y(\text{nearY}(u'_3)) - \varepsilon$. For u_3 , we assign $x(u_3) = x(u_2)$ and $y(u_3) = y(u_4)$. See Fig. 10a. Observe that Γ' is a planar drawing of G^\rightarrow . Similarly to the proof of Lemma 1, we can prove that u_3 and

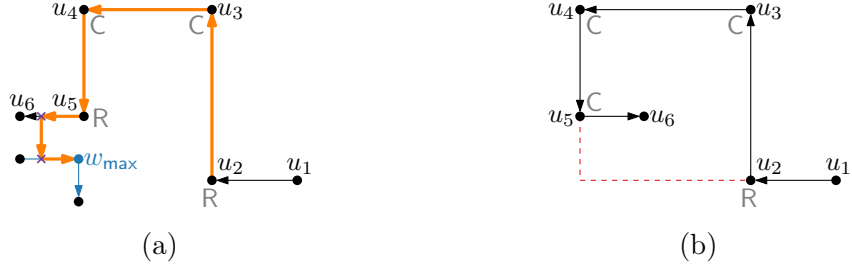


Figure 11: An illustration for cases considered in the proofs of (a) Lemma 3 and (b) Lemma 4. A path from u_2 to w_{\max} , to show that they are a pair of kitty corners, is drawn in orange.

near $\mathbb{Y}(u'_3)$ (which is also a vertex of G^\rightarrow) make a pair of kitty corner on the outer face of H (see Fig. 10b), a contradiction to the fact that the path that we are reducing does not contain any kitty corner. \square

We will next give our reduction rules for paths labeled RCCR, CRRC, RCCC, CCCR, CRRR and RRRC. Towards that, we give some properties of the drawing of these paths in any drawing of G^\rightarrow . We first consider a path labeled RCCR.

Lemma 3. *Suppose that there exists a path $P = (u_1, u_2, u_3, u_4, u_5, u_6)$ in G^\rightarrow such that $\text{label}(u_2) = \text{label}(u_5) = \text{R}$ and $\text{label}(u_3) = \text{label}(u_4) = \text{C}$. For any drawing Γ of G^\rightarrow , there exists another drawing Γ' of G^\rightarrow whose bounding box is the same as that of Γ and such that $y(u_2) = y(u_5)$ in Γ' .*

Proof. Let Γ be a drawing of G^\rightarrow . Assume that either $y(u_2) < y(u_5)$ or $y(u_5) < y(u_2)$ in Γ , else we are done (set $\Gamma' = \Gamma$). Specifically, we assume that $y(u_2) < y(u_5)$, since the case when $y(u_5) < y(u_2)$ is symmetric.

Observe that we can assume that there exists a vertex w such that $x(w) \in [x(u_6), x(u_5)]$ and $y(w) = y(u_5) - 1$, since otherwise we can shift u_5 and u_6 downwards. As $y(u_2) < y(u_5)$, $y(u_2) \leq y(w)$. Let S be the set of all such vertices w . Let w_{\max} be the vertex in S such that $x(w_{\max}) = \max\{x(w) \mid w \in S\}$. Observe that by Observation 2 and Lemma 1, if there exists a vertex z such that $x(z) \in [x(u_5), x(u_2)]$, $y(z) \in [y(u_2), y(u_3)]$ and $\text{prev}(z), \text{next}(z) \notin \{u_2, u_4\}$, then u_2 is a kitty corner of H . Therefore, there cannot be any such vertex z , as the path that we are reducing does not contain any kitty corner. Due to this, the neighbors of w_{\max} are to the left of and below w_{\max} . Moreover, from the planarity of Γ , we get that $\text{label}(w_{\max}) = \text{R}$.

Similarly to the proof of [Lemma 1](#), we can prove that (w_{\max}, u_2) is a pair of kitty corners of H , again a contradiction to the fact that the path that we are reducing does not contain any kitty corner. See [Fig. 11a](#). This, in turn, implies that $y(u_5) = y(u_2)$ in Γ or we can get another drawing Γ' of G^\rightarrow where we can shift u_5 and u_6 downwards such that $y(u_5) = y(u_2)$. \square

A lemma similar to [Lemma 3](#) for a path labeled CRRC is given as [Lemma 9](#) in the [Appendix](#).

We now give the following lemma for a path labeled RCCC or CCCR.

Lemma 4. *Suppose that there exists a path $P = (u_1, u_2, u_3, u_4, u_5, u_6)$ in G^\rightarrow such that $\text{label}(u_2) = R$ and $\text{label}(u_3) = \text{label}(u_4) = \text{label}(u_5) = C$ (resp., $\text{label}(u_2) = \text{label}(u_3) = \text{label}(u_4) = C$ and $\text{label}(u_5) = R$). For any drawing Γ of G^\rightarrow , $y(u_5) < y(u_2)$ in Γ .*

Proof. We will prove the lemma for the RCCC case. The proof for the other case is symmetric. Let Γ be a drawing of G^\rightarrow . Assume for contradiction that $y(u_2) \leq y(u_5)$. Then, $x(u_6) = x(u_5) + 1$ and $y(u_6) \in [y(u_2), y(u_4)]$. Moreover, $\text{prev}(u_6), \text{next}(u_6) \notin \{u_2, u_4\}$. Then, by [Observation 2](#) and [Lemma 1](#), $\text{nearY}(u_3)$ exists and $(\text{nearY}(u_3), u_2)$ is a kitty corner pair of H , a contradiction to the fact that the path that we are reducing does not contain any kitty corner. See [Fig. 11b](#). This implies that $y(u_5) < y(u_2)$ in Γ . \square

A lemma similar to [Lemma 4](#) for paths labeled CRRR or RRRC is given as [Lemma 10](#) in the [Appendix](#).

We now give the reduction rules for paths labeled RCCC, CCCR, CRRR and RRRC, followed by those for paths labeled RCCR and CRRC. We start by giving the reduction rule for RCCC. Recall that, due to previous reduction rules, there is no F-vertex or a path labeled RCR or CRC in G^\rightarrow .

Reduction Rule 3. *Suppose that there exists a path $P = (u_1, u_2, u_3, u_4, u_5, u_6)$ in G^\rightarrow such that $\text{label}(u_2) = R$ and $\text{label}(u_3) = \text{label}(u_4) = \text{label}(u_5) = C$. Then, delete the vertices u_3 and u_4 and the edges incident to them from G^\rightarrow and add a new path (u_2, u'_3, u_5) to G^\rightarrow . Moreover, assign $\text{label}(u_2) = F$, $\text{label}(u'_3) = C$, $\text{weight}((u_2, u'_3)) = \text{weight}((u_3, u_4))$, $\text{weight}((\text{prev}(u_1), u_1)) = \max\{\text{weight}((u_2, u_3)), \text{weight}((\text{prev}(u_1), u_1))\}$, and $\text{weight}((u'_3, u_5)) = \max\{\text{weight}((u_4, u_5)) - \text{weight}((u_2, u_3)), 1\}$. The labels of all the remaining vertices and the weights of all the remaining edges stay the same. Let $G_{\text{red}}^\rightarrow$ be the reduced graph. See [Fig. 12](#).*

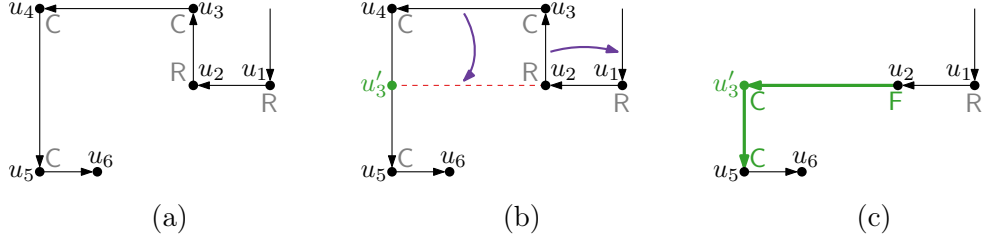


Figure 12: An illustration for Reduction Rule 3. The original path P is shown in (a) and the reduced path is shown in (c). (b) shows the vertex u'_3 , and the projection from the edges of $G^>$ that will be deleted when applying the reduction rule to the edges of $G^>_{\text{red}}$, represented by curved purple edges from an edge to be deleted to its projected edge.

Lemma 5. *Reduction Rule 3 is safe.*

Proof. To prove that Reduction Rule 3 is safe, we need to prove that there exists a planar drawing Γ of $G^>$ if and only if there exists a planar drawing Γ_{red} of $G^>_{\text{red}}$ such that Γ and Γ_{red} have the same bounding box. Recall that, without loss of generality, we assume that $\text{label}((u_1, u_2)) = W$.

(\Rightarrow) Let Γ be a planar drawing of $G^>$ having bounding box \mathcal{B} . By Lemma 4, we get that $y(u_5) < y(u_2)$ in Γ . As there is neither an F-vertex nor a path labeled CRC in $G^>$, we get that $\text{label}(u_1) = \text{R}$ and $\text{label}(\text{prev}(u_1))$ is either R or C. If $\text{label}(\text{prev}(u_1)) = \text{C}$, by Lemma 9, we get that there exists a drawing Γ' of $G^>$ (which may be the same as Γ) whose bounding box is \mathcal{B} such that $y(\text{prev}(u_1)) = y(u_3)$ in Γ' . Otherwise, we get that $\text{label}((\text{prev}(\text{prev}(u_1)), \text{prev}(u_1))) = \text{E}$. So, we can apply Lemma 9 after rotating the drawing Γ by 180° . This, in turn, implies that $y(u_3) < y(\text{prev}(u_1))$ in Γ . So, without loss of generality, we can assume that $y(u_5) < y(u_2)$ and $y(u_3) \leq y(\text{prev}(u_1))$.

We get a drawing Γ_{red} of $G^>_{\text{red}}$ having the same bounding box \mathcal{B} as follows. For every vertex $v \in V(G^>_{\text{red}}) \setminus \{u'_3\}$, $x(v)$ and $y(v)$ in Γ_{red} are the same as those in Γ . For u'_3 , we assign $x(u'_3) = x(u_4)$ and $y(u'_3) = y(u_2)$. Observe that as $y(u_5) < y(u_2)$ and $y(u'_3) = y(u_2)$, $y(u'_3) - y(u_5) \geq 1$. Moreover, $y(u_3) \leq y(\text{prev}(u_1))$. This implies that the weight constraints of the edges $(\text{prev}(u_1), u_1)$ and (u'_3, u_5) in $G^>_{\text{red}}$ are satisfied by Γ_{red} and \mathcal{B} is a bounding box of Γ_{red} . Moreover, if there does not exist any vertex $w \in V(G^>)$ such that $x(w) \in [x(u_4), x(u_2)]$ and $y(w) \in [y(u_2), y(u_4)]$ in Γ , Γ_{red} is a planar drawing of $G^>_{\text{red}}$. Assume for contradiction there exists such a w . Observe that

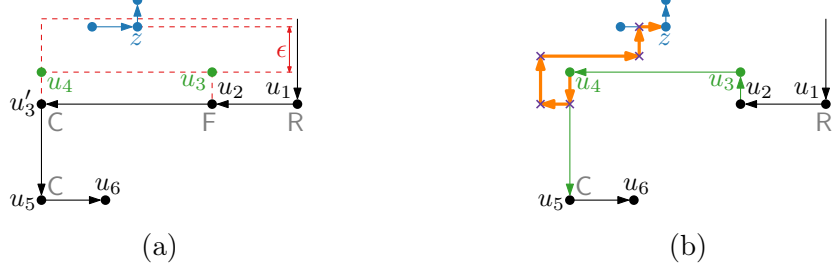


Figure 13: An illustration for the case considered in the reverse direction of the proof of Lemma 5. A path from u_4 to $\text{nearY}(u_1, \Gamma)$ (shown by z), to show that they are a pair of kitty corners, is drawn in orange.

$\text{prev}(w), \text{next}(w) \notin \{u_2, u_4\}$. Then, by Observation 2 and Lemma 1, $\text{nearY}(u_3)$ exists and $(\text{nearY}(u_3), u_2)$ is a kitty corner pair of H , a contradiction to the fact that the path that we are reducing does not contain any kitty corner.

(\Leftarrow) Let Γ_{red} be a planar drawing of $G_{\text{red}}^{\rightarrow}$ having bounding box \mathcal{B} . We get a drawing Γ of G^{\rightarrow} having the same bounding box \mathcal{B} as follows. For every vertex $v \in V(G^{\rightarrow}) \setminus \{u_3, u_4\}$, $x(v)$ and $y(v)$ in Γ are the same as those in Γ_{red} . For u_3 and u_4 , we assign $x(u_3) = x(u_2)$, $x(u_4) = x(u'_3)$ and $y(u_3) = y(u_4) = y(u_2) + \text{weight}((u_2, u_3))$. Observe that, as given in Reduction Rule 3, the weight of the edge $(\text{prev}(u_1), u_1)$ is the maximum of $\text{weight}((u_2, u_3))$ and $\text{weight}((\text{prev}(u_1), u_1))$, \mathcal{B} is a bounding box of Γ . Moreover, if there does not exist any vertex $w \in V(G_{\text{red}}^{\rightarrow})$ such that $x(w) \in [x(u'_3), x(u_2)]$ and $y(w) \in [y(u_2), y(u_2) + \text{weight}((u_2, u_3))]$ in Γ_{red} , then Γ is a planar drawing of G^{\rightarrow} . Assume for contradiction there exists such a w . Observe that $\text{prev}(w), \text{next}(w) \notin \{\text{prev}(u_1), u'_3\}$. Without loss of generality, for Observation 6, we can assume that u'_3 is the left neighbor of u_1 as $\text{label}(u_2) = \mathsf{F}$ in $G_{\text{red}}^{\rightarrow}$. Then, by Observation 6, $\text{nearY}(u_1)$ exists and $\text{label}(\text{nearY}(u_1)) = \mathsf{C}$. Let Γ' be a drawing of G^{\rightarrow} obtained from Γ_{red} as follows. Let $\varepsilon \in \mathbb{R}$ such that $0 < \varepsilon < 1$. For every vertex $v \in V(G^{\rightarrow}) \setminus \{u_3, u_4\}$, $x(v)$ and $y(v)$ in Γ' are the same as those in Γ_{red} . For u_3 and u_4 , we assign $x(u_3) = x(u_2)$, $x(u_4) = x(u'_3)$ and $y(u_3) = y(u_4) = y(\text{nearY}(u_1)) - \varepsilon$. See Fig. 13a. Observe that by the definition of $\text{nearY}(u_1)$, there exists no other vertex of $G_{\text{red}}^{\rightarrow}$ with x-coordinate in $[x(u'_3), x(u_1)]$ and y-coordinate smaller than that of $\text{nearY}(u_1)$ in Γ_{red} . Therefore, Γ' is a planar drawing of G^{\rightarrow} . Similarly to the proof of Lemma 1, we can prove that u_4 and $\text{nearY}(u_1)$ (which is also a vertex of G^{\rightarrow}) make a pair of kitty corner on the outer face of H (see Fig. 13b), a

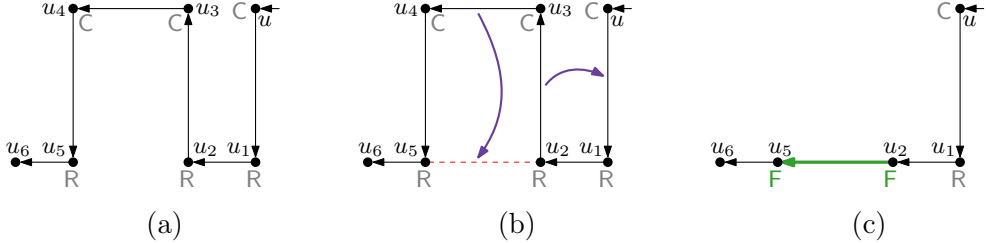


Figure 14: An illustration for Reduction Rule 4. The original path P is shown in (a) and the reduced path is shown in (c). (b) shows the projection from the edges of $G^>$ that will be deleted when applying the reduction rule to the edges of $G^>_{\text{red}}$, represented by curved purple edges from an edge to be deleted to its projected edge.

contradiction to the fact that the path that we are reducing does not contain any kitty corner. \square

As the reduction rules for paths labeled CCCR, CRRR, and RRRC are similar, they are provided as Reduction Rules 6–8 in the Appendix.

We now give the reduction rules for paths labeled RCCR or CRRC. We start by giving the reduction rule for RCCR. Recall that, due to previous reduction rules, there is neither an F-vertex nor a path labeled RCR, CRC, RCCC, CCCR, CRRR, or RRRC in $G^>$.

Reduction Rule 4. *Suppose that there exists a path $P = (u_1, u_2, u_3, u_4, u_5, u_6)$ in $G^>$ such that $\text{label}(u_2) = \text{label}(u_5) = \text{R}$ and $\text{label}(u_3) = \text{label}(u_4) = \text{C}$. Then, delete the vertices u_3 and u_4 and the edges incident to them from $G^>$ and add a new edge (u_2, u_5) to $G^>$. Moreover, assign $\text{label}(u_2) = \text{label}(u_5) = \text{F}$, $\text{weight}((u_2, u_5)) = \text{weight}((u_3, u_4))$ and $\text{weight}((\text{prev}(u_1), u_1)) = \max\{\text{weight}((u_2, u_3)), \text{weight}((\text{prev}(u_1), u_1))\}$. The labels of all the remaining vertices and the weights of all the remaining edges stay the same. Let $G^>_{\text{red}}$ be the reduced graph. See Fig. 14.*

Lemma 6. *Reduction Rule 4 is safe.*

Proof. To prove that Reduction Rule 4 is safe, we need to prove that there exists a planar drawing Γ of $G^>$ if and only if there exists a planar drawing Γ_{red} of $G^>_{\text{red}}$ such that Γ and Γ_{red} have the same bounding box. Recall that, without loss of generality, we assume that $\text{label}((u_1, u_2)) = W$.

(\Rightarrow) Let Γ be a planar drawing of G^\rightarrow having bounding box \mathcal{B} . By [Lemma 3](#), we get that $y(u_5) = y(u_2)$ in Γ . As there is neither an F -vertex nor a path labeled CRC or CRRR in G^\rightarrow , we get that $\mathsf{label}(u_1) = \mathsf{R}$ and $\mathsf{label}(\mathsf{prev}(u_1)) = \mathsf{C}$. By [Lemma 9](#), we get that $y(\mathsf{prev}(u_1)) = y(u_3)$. We get a drawing Γ_{red} of $G_{\mathsf{red}}^\rightarrow$ having the same bounding box \mathcal{B} as follows. For every vertex $v \in V(G_{\mathsf{red}}^\rightarrow)$, $x(v)$ and $y(v)$ in Γ_{red} are the same as those in Γ . Observe that $y(\mathsf{prev}(u_1)) = y(u_3)$ implies that the weight constraint of the edge $(\mathsf{prev}(u_1), u_1)$ in $G_{\mathsf{red}}^\rightarrow$ is satisfied by Γ_{red} and \mathcal{B} is a bounding box of Γ_{red} . Moreover, if there does not exist any vertex $w \in V(G^\rightarrow)$ such that $x(w) \in [x(u_4), x(u_2)]$ and $y(w) \in [y(u_2), y(u_4)]$ in Γ , then Γ_{red} is a planar drawing of $G_{\mathsf{red}}^\rightarrow$. Assume for contradiction there exists such a w . Observe that $\mathsf{prev}(w), \mathsf{next}(w) \notin \{u_2, u_4\}$. Then, by [Observation 2](#) and [Lemma 1](#), $\mathsf{nearY}(u_3)$ exists and $(\mathsf{nearY}(u_3), u_2)$ is a kitty corner pair of H , a contradiction to the fact that the path that we are reducing does not contain any kitty corner.

(\Leftarrow) Let Γ_{red} be a planar drawing of $G_{\mathsf{red}}^\rightarrow$ having bounding box \mathcal{B} . We get a drawing Γ of G^\rightarrow having the same bounding box \mathcal{B} as follows. For every vertex $v \in V(G^\rightarrow) \setminus \{u_3, u_4\}$, $x(v)$ and $y(v)$ in Γ are the same as those in Γ_{red} . For u_3 and u_4 , we assign $x(u_3) = x(u_2)$, $x(u_4) = x(u_5)$ and $y(u_3) = y(u_4) = y(u_2) + \mathsf{weight}((u_2, u_3))$. Observe that as $\mathsf{weight}((\mathsf{prev}(u_1), u_1)) = \max\{\mathsf{weight}((u_2, u_3)), \mathsf{weight}((\mathsf{prev}(u_1), u_1))\}$, \mathcal{B} is a bounding box of Γ . Moreover, if there does not exist any vertex $w \in V(G_{\mathsf{red}}^\rightarrow)$ such that $x(w) \in [x(u_5), x(u_2)]$ and $y(w) \in [y(u_2), y(u_2) + \mathsf{weight}((u_2, u_3))]$ in Γ_{red} , then Γ is a planar drawing of G^\rightarrow . Assume for contradiction there exists such a w . Observe that $\mathsf{prev}(w), \mathsf{next}(w) \notin \{\mathsf{prev}(u_1), u_6\}$. Without loss of generality, from [Observation 6](#), we can assume that u_6 is the left neighbor of u_1 as $\mathsf{label}(u_2) = \mathsf{label}(u_5) = \mathsf{F}$ in $G_{\mathsf{red}}^\rightarrow$. Then, by [Observation 6](#), $\mathsf{nearY}(u_1)$ exists and $\mathsf{label}(\mathsf{nearY}(u_1)) = \mathsf{C}$. Let Γ' be a drawing of G^\rightarrow obtained from Γ_{red} as follows. Let $\varepsilon \in \mathbb{R}$ such that $0 < \varepsilon < 1$. For every vertex $v \in V(G^\rightarrow) \setminus \{u_3, u_4\}$, $x(v)$ and $y(v)$ in Γ' are the same as those in Γ_{red} . For u_3 and u_4 , we assign $x(u_3) = x(u_2)$, $x(u_4) = x(u_5)$ and $y(u_3) = y(u_4) = y(\mathsf{nearY}(u_1)) - \varepsilon$. See [Fig. 15a](#). Observe that by the definition of $\mathsf{nearY}(u_1)$, there exists no other vertex of $G_{\mathsf{red}}^\rightarrow$ with x-coordinate in $[x(u_5), x(u_1)]$ and y-coordinate smaller than that of $\mathsf{nearY}(u_1)$ in Γ_{red} . Therefore, Γ' is a planar drawing of G^\rightarrow . Similar to the proof of [Lemma 1](#), we can prove that u_4 and $\mathsf{nearY}(u_1)$ (which is also a vertex of G^\rightarrow) make a pair of kitty corners on the outer face of H (see [Fig. 15b](#)), a contradiction to the fact that the path that we are reducing does not contain any kitty corner. \square

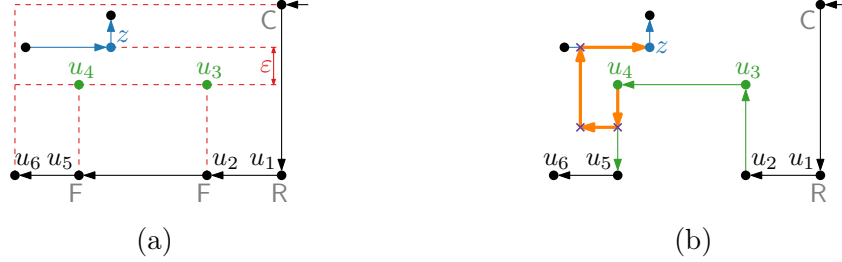


Figure 15: An illustration for the case considered in the reverse direction proof of Lemma 6. A path from u_4 to $\text{nearY}(u_1, \Gamma)$ (shown by z), to show that they are a pair of kitty corners, are drawn in orange.

As the reduction rule for a path labeled CRRC is similar, it is provided as Reduction Rule 9 in the Appendix.

Finally, to process a path labeled RRRRRR, we first define a matching $M_{RC}(G^\rightarrow)$ from the R-vertices to C-vertices in G^\rightarrow as follows. To define the matching, we first define the notion of a *balanced path*. Let u and v be two vertices of G^\rightarrow . We say that $P_{u,v}$ is *balanced* if the number of R-vertices is equal to the number of C-vertices in $P_{u,v}$. We have the following observation about a balanced path starting at an R-vertex, which will be useful in defining the matching.

Observation 3. *Let $P_{u,v}$ be a balanced path that starts with an R-vertex. Then, there exists a C-vertex x on this path such that $P_{u,x}$ is balanced.*

We now define the matching $M_{RC}(G^\rightarrow)$. Intuitively, in $M_{RC}(G^\rightarrow)$, every R-vertex u is matched to the closest C-vertex v such that every internal R-vertex on the path from u to v is mapped to an internal C-vertex on the path from u to v . Formally, we define $M_{RC}(G^\rightarrow)$ as a matching from the set of R-vertices to the set of C-vertices in G^\rightarrow as follows.

An R-vertex u is matched to a C-vertex v if and only if i) $P_{u,v}$ is balanced, and ii) for every internal C-vertex x of $P_{u,v}$, the path $P_{u,x}$ is not balanced. Observe that as the number of C-vertices is larger by 4 than the number of R-vertices, the matching $M_{RC}(G^\rightarrow)$ always exists. Moreover, it is also unique. See Fig. 16. In the following lemma, we also prove that if an R-vertex u is matched to a C-vertex v then every R-vertex on the path from u to v is matched to a C-vertex on the path from u to v .

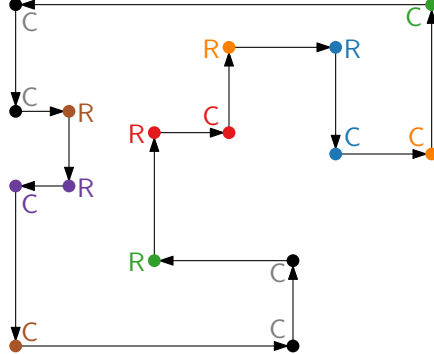


Figure 16: An illustration for the definition of the matching $M_{RC}(G^\rightarrow)$. The matched R- and C-vertex pairs are drawn in the same color and the remaining 4 unmatched C-vertices are drawn in black.

Lemma 7. *Let u be an R-vertex in G^\rightarrow . Moreover, let v be the C-vertex in G^\rightarrow that is matched to u by $M_{RC}(G^\rightarrow)$. Then, every R-vertex on the path $P_{u,v}$ is matched to a C-vertex on $P_{u,v}$ by $M_{RC}(G^\rightarrow)$.*

Proof. We prove the statement by induction on the number of vertices **num** of the path $P_{u,v}$. Observe that **num** is even as $P_{u,v}$ is balanced.

Base case (**num** = 2). When **num** = 2, $P_{u,v} = (u, v)$ such that **label**(u) = R and **label**(v) = C. As u is matched to v , the lemma is true for **num** = 2.

Inductive hypothesis. Suppose that the lemma is true for **num** = $2t \geq 2$.

Inductive step. We need to prove that the lemma is true for **num** = $2t + 2$. Let $P_{u,v} = (x_1 = u, x_2, \dots, x_{2t+1}, x_{2t+2} = v)$. Observe that **label**(x_2) = R, otherwise P_{u,x_2} is balanced, which contradicts property ii) of the definition of the matching. We now look at the path $P_{x_2,x_{2t+1}}$. Since $P_{u,v}$ is balanced, $P_{x_2,x_{2t+1}}$ is also balanced. Moreover, **label**(x_2) = R; so, by **Observation 3**, there exists a C-vertex x_i , for some $i \in [2, 2t + 1]$, such that P_{x_2,x_i} is balanced. Let $j \geq 2$ be the smallest such index for which P_{x_2,x_j} is balanced and **label**(x_j) = C. Due to the choice of j , for every internal C-vertex w of P_{x_2,x_j} , the path $P_{x_2,w}$ is not balanced. Therefore, by the definition of the matching, we get that x_2 is matched to x_j . As the number of vertices of P_{x_2,x_j} is at most $2t$, from the inductive hypothesis, we get that every R-vertex on P_{x_2,x_j} is matched to a C-vertex on P_{x_2,x_j} . Now, we remove the path P_{x_2,x_j} from $P_{u,v}$ and add an arc from u to x_{j+1} . Let P' be the resulting path. Then, P' is balanced (since we removed a balanced path), and property ii) is also true for P' as it

is true for $P_{u,v}$. Moreover, the number of vertices of P' is at most $2t$, so from the inductive hypothesis, we get the every R-vertex on P' is matched to a C-vertex on P' . This, in turn, implies that every R-vertex on $P_{u,v}$ is matched to a C-vertex on $P_{u,v}$. \square

We now consider a path (u_1, u_2, \dots, u_7) such that $\text{label}(u_i) = \text{R}$, for every $i \in [1, 7]$. Let v_i be the C-vertex that is matched to u_i by $M_{RC}(G^\rightarrow)$, for every $i \in [1, 7]$. Observe that by the property i) of the definition of $M_{RC}(G^\rightarrow)$, the number of R-vertices is equal to the number of C-vertices in P_{u_i, v_i} which implies that $\text{rot}(u_i, v_i) = -1$, for every $i \in [1, 7]$. Moreover, considering $u = u_6$ and $v = v_6$ in [Lemma 7](#), we get that $(u_6, u_7, \dots, v_7, \dots, v_6)$ is a path in G^\rightarrow . Thus, by recursively applying the same argument to u_5, u_4, \dots, u_1 , we get that $(u_1, u_2, u_3, u_4, u_5, u_6, u_7, \dots, v_7, \dots, v_6, \dots, v_5, \dots, v_4, \dots, v_3, \dots, v_2, \dots, v_1)$ is a path in G^\rightarrow . Therefore $\text{rot}(u_1, v_1) = \text{rot}(u_1, u_7) + \text{rot}(u_7, v_7) + \text{rot}(v_7, v_1) \Rightarrow \text{rot}(v_7, v_1) = 6$. As every C-vertex is a reflex vertex on the outer face f_{out} of G^\rightarrow , $\text{rot}(v_1, v_7) = -6$ on f_{out} . This, in turn, implies that v_1 and v_7 are a pair of kitty corners of f_{out} . Based on this matching $M_{RC}(G^\rightarrow)$, we give the following counting rule to count the vertices of a path on R-vertices having 7 or more vertices.

Counting Rule 1. *Let $k \in \mathbb{N}$ and $t \in [0, 6]$. Let $P = (u_1, u_2, \dots, u_{7k+t})$ be a maximal path on R-vertices in G^\rightarrow not containing any kitty corner, i.e., $\text{label}(u_i) = \text{R}$ and u_i is not a kitty corner of H , for every $i \in [1, 7k+t]$. Let v_i be the C-vertex matched to u_i by $M_{RC}(G^\rightarrow)$. Then, we count the set of vertices of P against the set of kitty corners $S_P = \{v_1, v_7, v_8, v_{14}, \dots, v_{7k-6}, v_{7k}\}$.*

Note that, for every maximal path P on R-vertices having 7 or more vertices, the set S_P is unique. Moreover, if two such maximal paths P_1 and P_2 are different, then they are also vertex-disjoint and it holds that $S_{P_1} \cap S_{P_2} = \emptyset$. Therefore, by the above counting rule, the total number of occurrences of R-vertices in G^\rightarrow that belong to maximal paths P on R-vertices having 7 or more vertices and not containing any kitty corner is bounded by a function that is linear in the number of kitty corners of H .

By applying all the reduction rules in their respective order until they can no longer be applied, from [Observation 1](#), we get that $P_{c_i, c_{i+1}}^{\text{trun}}$ only contains R-vertices and no kitty corner, for every $i \in [1, k]$. By applying [Counting Rule 1](#), the number of vertices of all such paths is bounded by a function that is linear in the number of kitty corners of H . As the number of vertices of every path $P_{c_i, c_{i+1}}$ is 10 more than $P_{c_i, c_{i+1}}^{\text{trun}}$, we get an instance I of the

WEIGHTED OC problem such that the number of vertices of I is bounded by a function that is linear in the number of kitty corners of H . To show that it is a compression, we also need to prove that the sizes of the edge weights of I (when encoded in binary) are bounded by a function that is linear in k . Observe that the weight of any edge of I is at most n , the number of vertices of G^\rightarrow . Therefore, if the sizes of the edge weights of I (when encoded in binary) are not bounded by a function that is linear in k , we get that $k = O(\log n)$. In this case, by [Theorem 1](#), we can solve the OC problem on G in $n^{O(1)}$ time. So, without loss of generality, we assume that $k = \Omega(\log n)$. This, in turn, implies that the size of I is bounded by a function that is polynomial in the number of kitty corners of H . Thus we get a polynomial compression (with a linear number of vertices) parameterized by the number of kitty corners of H . Moreover, if $k = \Omega(\log n)$, the WEIGHTED OC problem on cycle graphs is in NP due to the fact that we can always guess the length of each edge in the drawing (the number of guesses and the size of each number, that is, length, to guess are polynomial in n). As the OC problem on cycle graphs is NP-hard [5], we can exploit the following proposition given in the book of Fomin et al. [30] and conclude the proof of [Theorem 2](#).

Proposition 1 ([30], Theorem 1.6). *Let $Q \subseteq \Sigma^* \times \mathbb{N}$ be a parameterized language, and let $R \subseteq \Sigma^*$ be a language such that the unparameterized version of $Q \subseteq \Sigma^* \times \mathbb{N}$ is NP-hard and $R \subseteq \Sigma^*$ is in NP. If there is a polynomial compression of Q into R , then Q admits a polynomial kernel.*

5. Maximum Face Degree: Parameterized Hardness

We show that the OC problem remains NP-hard even if all faces have constant degrees. Our proof elaborates on the ideas of Patrignani's NP-hardness proof for OC [4], which we will recall in the following.

Let $\phi = (\mathcal{X}, \mathcal{C})$ be a SAT instance with variables $\mathcal{X} = X_1, \dots, X_n$ and clauses $\mathcal{C} = C_1, \dots, C_m$. Patrignani creates a graph G_ϕ with rectilinear representation H_ϕ and two variables $w_\phi = 9n + 4$ and $h_\phi = 9m + 7$ such that H_ϕ admits an orthogonal grid drawing of size $w_\phi \cdot h_\phi$ if and only if ϕ is satisfiable. On a high level, the reduction works as follows.

The outer face of H_ϕ (the *frame*) is a rectangle that requires width w_ϕ and height h_ϕ in its most compact drawing; see [Fig. 17](#). Inside the frame, every variable is represented by a rectangular region (the *variable rectangle*) of width 7 and height $h_\phi - 7$. Each variable rectangle is bounded from above

and below by a horizontal path, but not necessarily from the left and the right, as the clause gadgets will be laid through them. The variable rectangles are connected horizontally with *hinges* (short vertical paths) between them. Between the frame and the rectangles, there is a *belt*: a long path of $16n + 4$ vertices that consists of alternating subsequences of 4 reflex vertices followed by 4 convex vertices. The belt and the hinges make sure that every variable rectangle has to be drawn with exactly width 7 and height $h_\phi - 7$, while the belt also ensures that every variable rectangle is either shifted to the top (which represents a **true** variable assignment) or to the bottom (which represents a **false** variable assignment) of the rectangle.

Every clause is represented by a *chamber* through the variable rectangles; see Fig. 18. The chambers divide the variable rectangles evenly into m subrectangles of height 9, the *variable-clause rectangles*, with a height-2 connection between the rectangles; the height of the connection is ensured by further hinges above and below it. Depending on the truth-assignments of the variables, the variable-clause rectangles are either shifted up or shifted down by 3. Into each variable-clause rectangle, one or two *blocker rectangles* of width 1 are inserted, centered horizontally: if the corresponding variable does not appear in the clause, then a rectangle of height 7 at the top; if the variable appears negated, then a rectangle of height 2 at the top and a rectangle of height 5 at the bottom; and if the variable appears unnegated, then a rectangle of height 5 at the top and a rectangle of height 2 at the bottom. Into the chamber, a *pathway* that consists of $2n - 1$ *A-shapes* linked together by a horizontal segment is inserted. Each of the A-shapes can reside in the left or right half of a variable-clause rectangle. Since there are n variable-clause

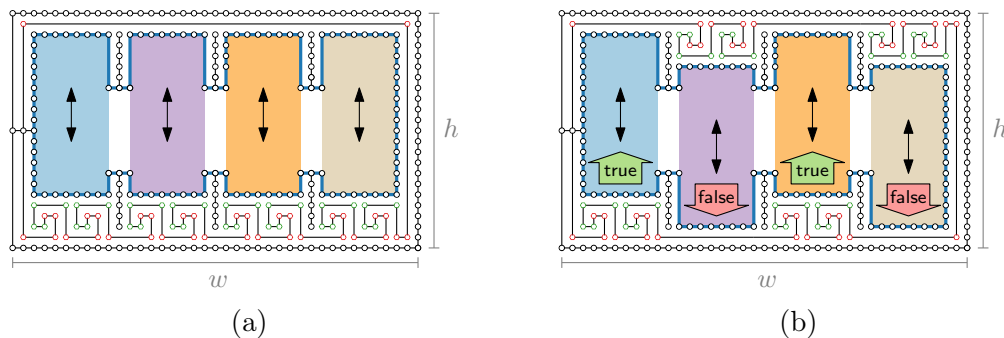


Figure 17: The shifting variable rectangles (shaded) and the belt (the path with hexagonal vertices) in the NP-hardness proof by Patrignani [4].

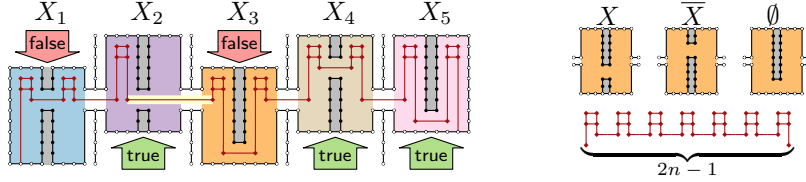


Figure 18: A clause gadget in the NP-hardness proof by Patrignani [4] for the clause $\overline{X_1} \vee X_2 \vee \overline{X_4}$: the variable-clause rectangles (color shaded), the blocking rectangles (gray shaded), and the pathway (the path with diamond vertices). The segment that corresponds to a fulfilled variable assignment for this clause (X_2) is highlighted.

rectangles, one half of such a rectangle remains empty; hence, one horizontal segment of the pathway has to pass a blocker rectangle, one half of a variable-clause rectangle, and the connection between two variable-clause rectangles. Thus, there must be one variable-clause rectangle where the opening between the blocker rectangle and the opening to the previous/next variable-clause rectangle are aligned vertically, which is exactly the case if the corresponding variable fulfills its truth assignment in the corresponding clause. For a full reduction, see Fig. 19.

Theorem 3. *OC* is para-NP-hard when parameterized by the maximum face degree.

Proof. To prove this theorem, we describe how to adjust Patrignani’s reduction such that every face has constant size, thus creating a graph G'_ϕ that has a constant maximum face degree with rectilinear representation H'_ϕ and two variables w'_ϕ and h'_ϕ such that H'_ϕ admits an orthogonal grid drawing of size $w'_\phi \cdot h'_\phi$ if and only if ϕ is satisfiable.

We start with the clause gadgets. Observe that the chamber consists of two large faces of size $O(m)$: above the pathway and below the pathway. To avoid these large faces, we seek to connect the pathway to the boundary of each of the variable-clause rectangles; once at the top and once at the bottom; see Fig. 20. To achieve this, we first increase the width of all variable-clause rectangles by 2 and their height by 4. The height of the connection between the rectangles is increased to 4. In each variable-clause rectangle, the height of the top blocking rectangle is increased by 3, thus increasing the height of the opening between/below them to 3. The larger openings are required for the connections from the pathway to the boundary of the variable-clause

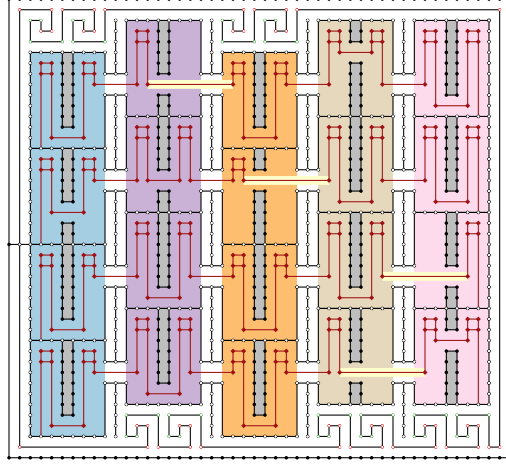


Figure 19: The full reduction by Patrignani [4] for the formula $(X_2 \vee \overline{X_4}) \wedge (X_1 \vee X_2 \vee \overline{X_3}) \wedge (X_5) \wedge (X_4 \vee \overline{X_5})$ with variable assignment $X_1 = X_3 = \text{false}$ and $X_2 = X_4 = X_5 = \text{true}$.

rectangles. We have to make sure that the A-shapes of the pathway still have to reside completely inside one half of a variable-clause rectangle. To achieve this, we also increase the necessary heights of the A-shapes by adding to more vertices to the vertical segments of their top square. Now, the top part of each A-shape is a rectangle of height at least 3, so it does not fit into any of the openings with size 3 or 4 without overlaps. We also add a vertex to the first and last vertical segment of the A-shape that we will use to connect to the variable-clause rectangles later.

We seek to connect every second A-shape to the top and bottom boundary of a variable-clause rectangle; namely, the $2i$ -th A-shape of the pathway shall be connected to the variable-clause rectangle corresponding to variable X_i , $1 \leq i \leq n - 1$. In particular, we always want to connect to the part to the right of the blocking rectangle. However, we do not know exactly which of the vertices to connect to, as it depends on whether the A-shape is placed inside the same variable-clause rectangle or in the next one. Hence, we remove all vertices (except the corner vertices and those on the blocking rectangles) from the top and bottom boundary of the variable-clause rectangles, and add a single *connector vertex* between the right corner and the blocking rectangle, if it exists, or between the right and the left corner, otherwise. To make sure that the variable-clause rectangles still have the required width and that the blocking rectangles are placed in the middle, we add a path of length 11

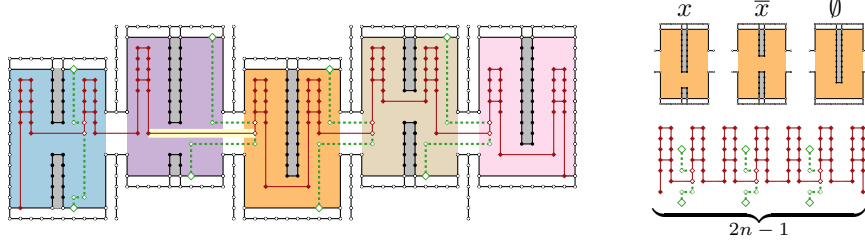


Figure 20: A clause gadget in our adjusted proof for the same clause and variable assignments as in Fig. 18. The connector vertices are drawn as large (green) unfilled diamonds.

(consisting of two vertical and nine horizontal segments) above and below the variable-clause rectangles, and connect the two middle vertices of the path to the blocking rectangle (if it exists).

Consider now the $2i$ -th A-shape and the i -th variable-clause gadget; refer again to Fig. 20. We connect the first vertex of the A-shape to the bottom connector vertex by a path of length 3 that consists of a vertical downwards segment, followed by a horizontal leftwards segment and a vertical downwards segment. We connect the second vertex of the A-shape to the top connector vertex by a path of length 2 that consists of a horizontal leftwards segment followed by a vertical upwards segment. If the A-shape lies in the i -th variable clause gadget, then it lies in the right half of it. Since we increase the width of the rectangle, this half has width 3 and thus there is enough horizontal space for the connections if the A-shape is drawn as far right as possible. Also, since the opening between/below the blocking rectangles has height 2, there is enough vertical space between the A-shape and the bottom connector if the horizontal segment to the $(2i-1)$ -th A-shape is drawn as far up as possible. On the other hand, if the A-shape lies in the $(i+1)$ -th variable clause gadget, then it lies in the left half of it. Since the opening between the variable-clause rectangles now has height 3, there is enough vertical space to fit the the connection to the $(2i-1)$ -th A-shape as well as the horizontal segment on the path to the connector vertices through the opening, and if the A-shape that lies in the right half of the i -th variable-clause rectangle is drawn as far left as possible, then there is also enough horizontal space to fit the vertical connection.

We still have to make sure that one half of a variable-clause rectangle can be “skipped” by the pathway if and only if the truth-assignment of a

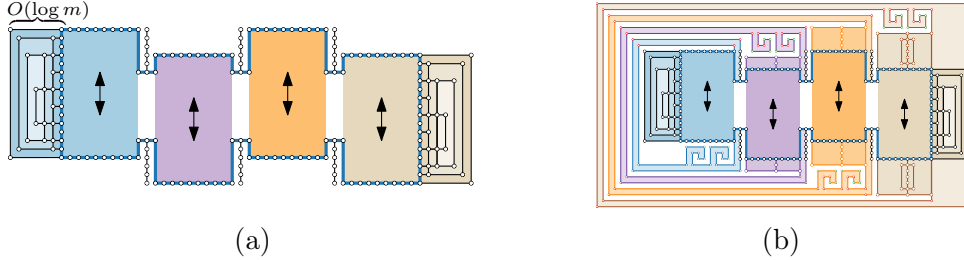


Figure 21: The frame in our adjusted NP-hardness reduction. (a) The left and right extensions of the first and last variable rectangle; (b) the belts around the variable rectangles.

variable is fulfilled in the corresponding clause. We increase the lengths of the top hinges by 3 and the lengths of the bottom hinges by 1. This ensures that the opening of the connections has height 4 as required, and that a horizontal segment can pass through a connection and a blocking rectangle opening if and only if a variable is variable rectangle is shifted down (the variable is assigned `false`) and the variable appears negated in the clause, or if a variable is shifted up (the variable is assigned `false`) and the variable appears unnegated in the clause, therefore satisfying our requirements. Furthermore, observe that each face in the clause gadget now has degree at most 55: there are at most 25 vertices from the pathway (2 A-shapes + 1 vertex), at most 18 vertices from a blocking rectangle, at most 6 vertices from the paths to (including) the connector vertices, and at most 6 vertices from the boundary of the chamber.

We now consider the frame and the variable rectangles. There are three large faces: the outer face, the face between the frame and the belt, and the face between the belt and the variable rectangles; all of these have degree $\Theta(n + m)$.

We first show how to deal with the face between the variable rectangles and the belt. We ignore the belt for now and focus on the path around the variable rectangles; see Fig. 21. This path consists of two vertical paths of length $O(m)$ on the left and the right of the first and the last variable rectangle, respectively, and an x -monotone path of length $O(n)$ between them. Consider the vertical path on the left of the first variable rectangle, let $z \in O(m)$ be its length and pick some constant integer $c \geq 2$. We first place a rectangle to the left of the path by connecting the topmost with the bottommost vertex with a path of length 3, consisting of a horizontal leftward

segment followed by a vertical downward and a horizontal rightward segment. This creates a new interior rectangular face with 2 vertices on the left and z vertices on the right. We now iteratively decrease the degree of this face, adding new faces of degree 10 and rectangular faces of degree at most $c + 3$, until this face also has constant degree. We place at most z/c rectangles to the left of the right path, each of height at most c , by adding a vertical path of at most $z/c + 1$ vertices that are connected to the second vertex from the top, the second vertex from the bottom, and every c -th vertex in between. This way, we create at most z/c new faces of degree at most $c + 3$, and a new vertical path of length at most $z/c + 1$. We connect the topmost and the bottommost vertex of this new path to create a new rectangular face as before. This creates a C-shaped face of degree 10, and a new interior rectangular face with two vertices on the left and at most $z/c + 1$ vertices on the right. We repeat this process at most $\log_c(z) + 1$ times, until the vertical path on the right has length at most c and thus the interior face has degree at most $c + 6$; see [Fig. 21a](#). We do the same to the vertical path on the right of the last variable rectangle. This way, we create at most $2z$ new faces, all of constant degree, and the full path now has length $O(n)$.

Instead of placing a single belt and outer face, we now add a small belt of only 20 vertices around every variable rectangle. Namely, the belt starts and ends at the rightmost vertex of the top and bottom boundary of the variable rectangles, respectively. For the first variable rectangle, the belt bounds a face of at most $30 + c$ vertices: 20 from the belt, 10 from the top, and c from the extension to the left. We add another path between the extreme vertices of the hinges between the variable rectangles that consists of four 90° -vertices; this creates a face of degree 40: 4 from this path, 20 from the belt, 10 from the hinges, and 6 from the variable rectangles. This path also functions as a bounding box for the belt: the minimum bounding box for this path can only be achieved if both spirals of the belt are either below or above the variable rectangle, thus creating the binary choice of shifting the variable rectangle up (**true**) or down (**false**).

For the next variable rectangles, we have to be a bit more careful. Repeating the process as for the first variable rectangle does not immediately work, as the new belt has to walk around the path that describes the bounding box for the previous variable rectangle plus its belt. Thus, there would be a gap of height 2 above and below the variable rectangle. This means that the variable rectangle could shift up- and downwards by two coordinates, which makes the clause gadgets invalid. To avoid this issue and to close the gap, we

place a box of height 2 above and below the second variable rectangle, and we place a box of height $2(i - 1)$ around the i -th variable rectangle, for each $i \in \{3, \dots, n\}$. To avoid a face of degree $O(n)$, we use the same strategy as for the leftmost path of the left variable gadget: we place a rectangle with an interior vertical path of height $2(i - 1)$ and we keep refining the resulting faces until they all have constant degree. This way, we create $2(n - 1)$ faces of degree at most 46: 20 from the belt, 4 from the bounding box path, 10 from the hinges, 6 from the vertical extension boxes, and 6 from the variable rectangles. The outer face of the graph has only degree 6: four from the bounding box, and the two corners of the rightwards extension of the last variable rectangle.

With this adjustment, we can still encode the variable assignments of a variable rectangle being either shifted up (`true`) or down (`false`), and we can draw the rectilinear representation with minimum width and height if and only if every clause gadget has a compact drawing, thus the whole rectilinear representation has an orthogonal drawing with area $w'_\phi \times h'_\phi$ for some fixed width w'_ϕ and height h'_ϕ if and only if ϕ is satisfiable. Clearly, w'_ϕ and h'_ϕ (and the number of vertices) are polynomial in n and m , and as described above all faces have constant degree.

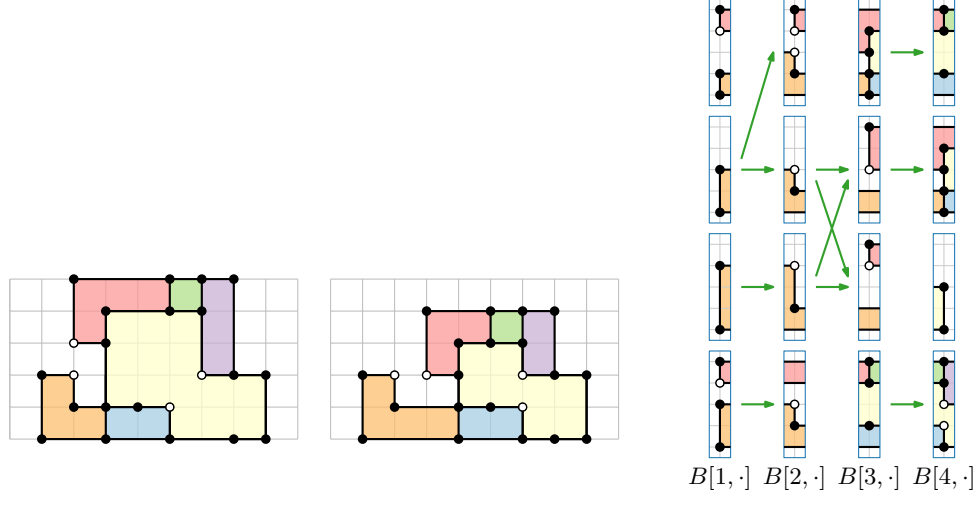
Hence, OC remains NP-hard even for graphs of constant face degree and thus it is para-NP-hard when parameterized by the maximum face degree. \square

6. Height of the Representation: An XP Algorithm

Given a connected planar graph G of vertex-degree at most 4, recall that the *height* of a rectilinear representation H of G is the minimum height of a rectangular section of the integer grid required to draw H orthogonally. By “guessing” for every column of the drawing what lies on each grid point, we obtain an XP algorithm for OC parameterized by the height of the representation.

Theorem 4. *Given a connected planar graph G , a rectilinear representation H of G with n vertices, and an integer $h \geq 1$, we can decide, in $n^{O(h)}$ time, whether H admits an orthogonal drawing of height h . In other words, OC is XP with respect to h .*

Proof. We want to decide whether H admits an orthogonal drawing on a grid that consists of h horizontal lines. Given a solution, that is, a drawing of H , we can remove any column that does not contain any vertex. Hence it



(a) two drawings of the same orthogonal representation (b) part of the DP table

Figure 22: Part of the table (b) used by our DP for checking whether the orthogonal representation depicted in (a) admits a drawing of height 5. The arcs that enter an entry $B[c, t]$ come from the entries that are taken into account when computing $B[c, t]$. The white vertices are part of a pair of kitty corners.

suffices to check whether there exists a drawing of H on a grid of (height h and) width $w \leq n$.

To this end, we use dynamic programming (DP) with a table B . Each entry of $B[c, t]$ corresponds to a column c of the grid and an h -tuple t . For an example, see Fig. 22b. Each component of t represents an object (if any) that lies on the corresponding grid point in column c . In a drawing of H , a grid point g can either be empty or it is occupied by a vertex or by an edge. In the case of an edge, the edge can pass through g either horizontally or vertically, as prescribed by H . Let \mathcal{T} be the set of h -tuples constructed in this way. Due to our observation regarding w above, \mathcal{T} does not contain any h -tuple that consists exclusively of horizontally crossing edges and empty grid points. Hence $|\mathcal{T}| \in (O(n))^h$.

Observe that, in an orthogonal drawing, each column can be considered a *cut* of the graph that the drawing represents. Hence, any $t \in \mathcal{T}$ uniquely defines all elements of H that, in any height- h grid drawing, cross c or lie to the left of c . We refer to this part of H as $\text{left}_H(t)$. Analogously, we define the set $\text{on}_H(t)$ as the elements that are encoded by t , that is, vertices or

edges of H that lie on the corresponding grid column, or edges that cross the column. Note that every horizontal edge in $\mathbf{on}_H(t)$ is also contained in $\mathbf{left}_H(t)$, whereas every vertical edge in $\mathbf{on}_H(t)$ is *not* contained in $\mathbf{left}_H(t)$. The table entry $B[c, t]$ stores a Boolean value that is true if an orthogonal drawing of $\mathbf{left}_H(t)$ on a grid of size $c \times h$ (counting grid lines) exists, false otherwise.

We fill the table $B[\cdot, \cdot]$ from left to right, that is, in order of increasing first component. If $c = 1$, we check, for each $t \in \mathcal{T}$, whether $\mathbf{left}_H(t) = \emptyset$. In this case, we set $B[1, t] = \mathbf{true}$, otherwise to \mathbf{false} . For the case $c > 1$, we define $t' \in \mathcal{T}$ to be a *direct predecessor* of $t \in \mathcal{T}$ if $\mathbf{left}_H(t) = \mathbf{left}_H(t') \cup \mathbf{on}_H(t')$ and, if we place t' on a column directly in front of t , they “match”, that is, every edge that starts in t' or crosses t' either ends on t or crosses t (in the same row in t and t'). In particular, edges that cross both columns must lie in the same row. For every $t \in \mathcal{T}$, we set $B[c, t] = \mathbf{true}$ if t has a direct predecessor t' such that $B[c - 1, t'] = \mathbf{true}$. Otherwise, we set $B[c, t] = \mathbf{false}$.

The DP returns \mathbf{true} if and only if there exists a pair $(c, t) \in [w] \times \mathcal{T}$ such that $B[c, t] = \mathbf{true}$ and $\mathbf{left}_H(t) \cup \mathbf{on}_H(t) = V(H) \cup E(H)$.

The number of different h -tuples is $(O(n))^h$. For each $(c, t) \in [w] \times \mathcal{T}$, we can compute $B[c, t]$ in $O(h) \cdot (O(n))^h$ time. Hence, the DP runs in $n^{O(h)}$ total time. \square

7. Conclusions and Open Problems

In this paper we studied the problem of computing an orthogonal drawing of a given orthogonal representation such that the area of the drawing is minimized. While the problem is known to be NP-complete in general, we show that it is FPT when parameterized by the number of kitty corners and that, if the graph is a simple cycle, there is a kernel of polynomial size. We also considered parameters other than the number of kitty corners: We proved that it remains NP-hard when parameterized by the maximum face degree, and showed the existence of an XP algorithm when the parameter is the height of the drawing. We conclude by listing some open problems that, in our opinion, can be the subject of further investigation.

- (1) Can we find a polynomial kernel for OC with respect to the number of kitty corners, or at least with respect to the number of kitty corners plus the number of faces, for general graphs?
- (2) Does OC admit an FPT algorithm parameterized by the height of the orthogonal representation?

- (3) Is OC solvable in $2^{O(\sqrt{n})}$ time? This bound would be tight assuming that the Exponential Time Hypothesis is true.
- (4) If we parameterize by the number of *pairs* of kitty corners, can we achieve substantially better running times?
- (5) Can we substantially reduce the base of the exponent in the running time of the FPT algorithm? In particular, is the problem solvable in time $c^k \cdot n^{O(1)}$ for $c < 10$?

Acknowledgements. This research was initiated at Dagstuhl Seminar 21293: *Parameterized Complexity in Graph Drawing*. We are grateful to the organizers for making the seminar possible and to the other participants for useful discussions.

References

- [1] G. Di Battista, P. Eades, R. Tamassia, I. G. Tollis, Graph Drawing: Algorithms for the Visualization of Graphs, Prentice-Hall, 1999.
- [2] M. Kaufmann, D. Wagner (Eds.), Drawing Graphs, Methods and Models, Vol. 2025 of Lecture Notes in Computer Science, Springer, 2001. [doi:10.1007/3-540-44969-8](https://doi.org/10.1007/3-540-44969-8).
- [3] S. S. Bridgeman, G. Di Battista, W. Didimo, G. Liotta, R. Tamassia, L. Vismara, Turn-regularity and optimal area drawings of orthogonal representations, *Comput. Geom.* 16 (1) (2000) 53–93. [doi:10.1016/S0925-7721\(99\)00054-1](https://doi.org/10.1016/S0925-7721(99)00054-1).
- [4] M. Patrignani, On the complexity of orthogonal compaction, *Comput. Geom.* 19 (1) (2001) 47–67. [doi:10.1016/S0925-7721\(01\)00010-4](https://doi.org/10.1016/S0925-7721(01)00010-4).
- [5] W. S. Evans, K. Fleszar, P. Kindermann, N. Saeedi, C.-S. Shin, A. Wolff, Minimum rectilinear polygons for given angle sequences, *Comput. Geom.* 100 (101820) (2022) 1–39. [doi:10.1016/j.comgeo.2021.101820](https://doi.org/10.1016/j.comgeo.2021.101820).
- [6] M. J. Bannister, D. Eppstein, J. A. Simons, Inapproximability of orthogonal compaction, *J. Graph Algorithms Appl.* 16 (3) (2012) 651–673. [doi:10.7155/jgaa.00263](https://doi.org/10.7155/jgaa.00263).

- [7] R. Ganian, F. Montecchiani, M. Nöllenburg, M. Zehavi, Parameterized complexity in graph drawing (Dagstuhl Seminar 21293), *Dagstuhl Reports* 11 (6) (2021) 82–123. [doi:10.4230/DagRep.11.6.82](https://doi.org/10.4230/DagRep.11.6.82).
- [8] M. J. Bannister, D. Eppstein, Crossing minimization for 1-page and 2-page drawings of graphs with bounded treewidth, *J. Graph Algorithms Appl.* 22 (4) (2018) 577–606. [doi:10.7155/jgaa.00479](https://doi.org/10.7155/jgaa.00479).
- [9] S. Bhore, R. Ganian, F. Montecchiani, M. Nöllenburg, Parameterized algorithms for book embedding problems, *J. Graph Algorithms Appl.* 24 (4) (2020) 603–620. [doi:10.7155/jgaa.00526](https://doi.org/10.7155/jgaa.00526).
- [10] S. Bhore, R. Ganian, F. Montecchiani, M. Nöllenburg, Parameterized algorithms for queue layouts, *J. Graph Algorithms Appl.* 26 (3) (2022) 335–352. [doi:10.7155/JGAA.00597](https://doi.org/10.7155/JGAA.00597).
- [11] C. Binucci, G. Da Lozzo, E. Di Giacomo, W. Didimo, T. Mchedlidze, M. Patrignani, Upward book embeddings of st-graphs, in: G. Barequet, Y. Wang (Eds.), *Symp. Comput. Geom. (SoCG)*, Vol. 129 of LIPIcs, Schloss Dagstuhl – Leibniz-Zentrum für Informatik, 2019, pp. 13:1–13:22. [doi:10.4230/LIPIcs.SoCG.2019.13](https://doi.org/10.4230/LIPIcs.SoCG.2019.13).
- [12] Y. Kobayashi, H. Ohtsuka, H. Tamaki, An improved fixed-parameter algorithm for one-page crossing minimization, in: D. Lokshtanov, N. Nishimura (Eds.), *Int. Symp. Parametr. & Exact Comput. (IPEC)*, Vol. 89 of LIPIcs, Schloss Dagstuhl – Leibniz-Zentrum für Informatik, 2018, pp. 25:1–25:12. [doi:10.4230/LIPIcs.IPEC.2017.25](https://doi.org/10.4230/LIPIcs.IPEC.2017.25).
- [13] S. Chaplick, E. Di Giacomo, F. Frati, R. Ganian, C. N. Raftopoulou, K. Simonov, Parameterized algorithms for upward planarity, in: X. Goaoc, M. Kerber (Eds.), *Symp. Comput. Geom. (SoCG)*, Vol. 224 of LIPIcs, Schloss Dagstuhl – Leibniz-Zentrum für Informatik, 2022, pp. 26:1–26:16. [doi:10.4230/LIPIcs.SoCG.2022.26](https://doi.org/10.4230/LIPIcs.SoCG.2022.26).
- [14] E. Di Giacomo, G. Liotta, F. Montecchiani, Orthogonal planarity testing of bounded treewidth graphs, *J. Comput. Syst. Sci.* 125 (2022) 129–148. [doi:10.1016/j.jcss.2021.11.004](https://doi.org/10.1016/j.jcss.2021.11.004).
- [15] S. Gupta, G. Sa’ar, M. Zehavi, Grid recognition: Classical and parameterized computational perspectives, in: H.-K. Ahn, K. Sadakane

(Eds.), Int. Symp. Algorithms & Comput. (ISAAC), Vol. 212 of LIPIcs, Schloss Dagstuhl – Leibniz-Zentrum für Informatik, 2021, pp. 37:1–37:15. [doi:10.4230/LIPIcs.ISAAC.2021.37](https://doi.org/10.4230/LIPIcs.ISAAC.2021.37).

- [16] G. Da Lozzo, D. Eppstein, M. T. Goodrich, S. Gupta, Subexponential-time and FPT algorithms for embedded flat clustered planarity, in: A. Brandstädt, E. Köhler, K. Meer (Eds.), Int. Workshop Graph-Theoretic Concepts Comput. Sci. (WG), Vol. 11159 of LNCS, Springer, 2018, pp. 111–124. [doi:10.1007/978-3-030-00256-5_10](https://doi.org/10.1007/978-3-030-00256-5_10).
- [17] G. Liotta, I. Rutter, A. Tappini, Parameterized complexity of graph planarity with restricted cyclic orders, in: M. A. Bekos, M. Kaufmann (Eds.), Int. Workshop on Graph-Theoretic Concepts in Comput. Sci. (WG), Vol. 13453 of LNCS, Springer, 2022, pp. 383–397. [doi:10.1007/978-3-031-15914-5_28](https://doi.org/10.1007/978-3-031-15914-5_28).
- [18] G. Da Lozzo, D. Eppstein, M. T. Goodrich, S. Gupta, C-planarity testing of embedded clustered graphs with bounded dual carving-width, *Algorithmica* 83 (8) (2021) 2471–2502. [doi:10.1007/s00453-021-00839-2](https://doi.org/10.1007/s00453-021-00839-2).
- [19] M. J. Bannister, S. Cabello, D. Eppstein, Parameterized complexity of 1-planarity, *J. Graph Algorithms Appl.* 22 (1) (2018) 23–49. [doi:10.7155/jgaa.00457](https://doi.org/10.7155/jgaa.00457).
- [20] M. J. Bannister, D. Eppstein, J. A. Simons, Fixed parameter tractability of crossing minimization of almost-trees, in: S. Wismath, A. Wolff (Eds.), Int. Symp. Graph Drawing (GD), Vol. 8242 of LNCS, Springer, 2013, pp. 340–351. [doi:10.1007/978-3-319-03841-4_30](https://doi.org/10.1007/978-3-319-03841-4_30).
- [21] V. Dujmović, M. R. Fellows, M. Kitching, G. Liotta, C. McCartin, N. Nishimura, P. Ragde, F. A. Rosamond, S. Whitesides, D. R. Wood, On the parameterized complexity of layered graph drawing, *Algorithmica* 52 (2) (2008) 267–292. [doi:10.1007/s00453-007-9151-1](https://doi.org/10.1007/s00453-007-9151-1).
- [22] V. Dujmović, H. Fernau, M. Kaufmann, Fixed parameter algorithms for one-sided crossing minimization revisited, *J. Discrete Algorithms* 6 (2) (2008) 313–323. [doi:10.1016/j.jda.2006.12.008](https://doi.org/10.1016/j.jda.2006.12.008).
- [23] S. Cornelsen, G. Da Lozzo, L. Grilli, S. Gupta, J. Kratochvíl, A. Wolff, The parametrized complexity of the segment number, in: M. Bekos,

M. Chimani (Eds.), Int. Symp. Graph Drawing & Network Vis. (GD), Vol. 14466 of LNCS, Springer, 2023, pp. 97–113. [doi:10.1007/978-3-031-49275-4_7](https://doi.org/10.1007/978-3-031-49275-4_7).

- [24] S. Chaplick, K. Fleszar, F. Lipp, A. Ravsky, O. Verbitsky, A. Wolff, The complexity of drawing graphs on few lines and few planes, *J. Graph Algorithms Appl.* 27 (6) (2023) 459–488. [doi:10.7155/jgaa.00630](https://doi.org/10.7155/jgaa.00630).
- [25] M. Balko, S. Chaplick, R. Ganian, S. Gupta, M. Hoffmann, P. Valtr, A. Wolff, Bounding and computing obstacle numbers of graphs, *SIAM J. Discrete Math.* 38 (2) (2024) 1537–1565. [doi:10.1137/23M1585088](https://doi.org/10.1137/23M1585088).
- [26] T. C. Biedl, Small drawings of outerplanar graphs, series-parallel graphs, and other planar graphs, *Discret. Comput. Geom.* 45 (1) (2011) 141–160. [doi:10.1007/s00454-010-9310-z](https://doi.org/10.1007/s00454-010-9310-z).
- [27] S. Chaplick, K. Fleszar, F. Lipp, A. Ravsky, O. Verbitsky, A. Wolff, Drawing graphs on few lines and few planes, *J. Comput. Geom.* 11 (1) (2020) 433–475. [doi:10.20382/jocg.v11i1a17](https://doi.org/10.20382/jocg.v11i1a17).
- [28] M. Cygan, F. V. Fomin, L. Kowalik, D. Lokshtanov, D. Marx, M. Pilipczuk, M. Pilipczuk, S. Saurabh, *Parameterized Algorithms*, Springer, 2015. [doi:10.1007/978-3-319-21275-3](https://doi.org/10.1007/978-3-319-21275-3).
- [29] R. G. Downey, M. R. Fellows, *Fundamentals of Parameterized Complexity*, Vol. 4 of TCS, Springer, 2013. [doi:10.1007/978-1-4471-5559-1](https://doi.org/10.1007/978-1-4471-5559-1).
- [30] F. V. Fomin, D. Lokshtanov, S. Saurabh, M. Zehavi, *Kernelization: Theory of Parameterized Preprocessing*, Cambridge University Press, 2019.
- [31] G. Di Battista, R. Tamassia, Algorithms for plane representations of acyclic digraphs, *Theor. Comput. Sci.* 61 (1988) 175–198. [doi:10.1016/0304-3975\(88\)90123-5](https://doi.org/10.1016/0304-3975(88)90123-5).
- [32] P. Bertolazzi, G. Di Battista, G. Liotta, C. Mannino, Upward drawings of triconnected digraphs, *Algorithmica* 12 (6) (1994) 476–497. [doi:10.1007/BF01188716](https://doi.org/10.1007/BF01188716).
- [33] C. A. Pickover, *The Math Book*, Sterling, 2009.

- [34] J. L. Bentley, T. Ottmann, Algorithms for reporting and counting geometric intersections, *IEEE Trans. Comput.* C-28 (9) (1979) 643–647. [doi:10.1109/TC.1979.1675432](https://doi.org/10.1109/TC.1979.1675432).
- [35] M. I. Shamos, D. Hoey, Geometric intersection problems, in: *Symp. Foundat. Comput. Sci. (FoCS)*, 1976, pp. 208–215. [doi:10.1109/SFCS.1976.16](https://doi.org/10.1109/SFCS.1976.16).
- [36] R. Tamassia, On embedding a graph in the grid with the minimum number of bends, *SIAM J. Comput.* 16 (3) (1987) 421–444. [doi:10.1137/0216030](https://doi.org/10.1137/0216030).

Appendix

In this section, we provide the observations, reduction rules, and lemmas omitted in Section 4 to improve readability. We first give observations similar to Observation 2 for the cases when either $\text{right}(v)$ and $\text{below}(v)$ (Fig. 7b), or $\text{right}(v)$ and $\text{above}(v)$ (Fig. 7c), or $\text{left}(v)$ and $\text{above}(v)$ (Fig. 7d) exist.

Observation 4. *Let v be an R- or a C-vertex of G^\rightarrow such that $\text{right}(v)$ and $\text{below}(v)$ exist. Let Γ be a drawing of G^\rightarrow such that there exists a vertex u for which (i) $x(u) \in [x(\text{below}(v)), x(\text{right}(v))]$, (ii) $y(u) \in [y(\text{below}(v)), y(\text{right}(v))]$, and (iii) $u, \text{prev}(u), \text{next}(u) \notin \{\text{right}(v), \text{below}(v)\}$. Let S be the set of all such vertices. Let $\text{maxY} = \max\{y(v) \mid v \in S\}$ and $\text{minX} = \min\{x(v) \mid v \in S\}$.*

Then, $\text{nearX}(v, \Gamma)$ is the vertex in S such that $x(\text{nearX}(v, \Gamma)) = \text{minX}$ and $y(\text{nearX}(v, \Gamma)) = \max\{y(v) \mid v \in S \wedge x(v) = \text{minX}\}$. Similarly, $\text{nearY}(v, \Gamma)$ is the vertex in S such that $y(\text{nearY}(v, \Gamma)) = \text{maxY}$ and $x(\text{nearY}(v, \Gamma)) = \min\{x(v) \mid v \in S \wedge y(v) = \text{maxY}\}$. It follows from the definition that the neighbors of $\text{nearX}(v, \Gamma)$ (resp., $\text{nearY}(v, \Gamma)$) are to the right of and below $\text{nearX}(v, \Gamma)$ (resp., $\text{nearY}(v, \Gamma)$). Moreover, from the planarity of Γ , it follows that $\text{label}(\text{nearX}(v, \Gamma)) \in \{\text{R}, \text{C}\} \setminus \{\text{label}(v)\}$ and $\text{label}(\text{nearY}(v, \Gamma)) \in \{\text{R}, \text{C}\} \setminus \{\text{label}(v)\}$. See Fig. 7b.

Observation 5. *Let v be an R- or a C-vertex of G^\rightarrow such that $\text{right}(v)$ and $\text{above}(v)$ exist. Let Γ be a drawing of G^\rightarrow such that there exists a vertex u for which (i) $x(u) \in [x(\text{above}(v)), x(\text{right}(v))]$, (ii) $y(u) \in [y(\text{right}(v)), y(\text{above}(v))]$, and (iii) $u, \text{prev}(u), \text{next}(u) \notin \{\text{right}(v), \text{above}(v)\}$. Let S be the set of all such vertices. Let $\text{minY} = \min\{y(v) \mid v \in S\}$ and $\text{minX} = \min\{x(v) \mid v \in S\}$.*

Then, $\text{nearX}(v, \Gamma)$ is the vertex in S such that $x(\text{nearX}(v, \Gamma)) = \text{minX}$ and $y(\text{nearX}(v, \Gamma)) = \min\{y(v) \mid v \in S \wedge x(v) = \text{minX}\}$. Similarly, $\text{nearY}(v, \Gamma)$ is the vertex in S such that $y(\text{nearY}(v, \Gamma)) = \text{minY}$ and $x(\text{nearY}(v, \Gamma)) = \min\{x(v) \mid v \in S \wedge y(v) = \text{minY}\}$. It follows from the definition that the neighbors of $\text{nearX}(v, \Gamma)$ (resp., $\text{nearY}(v, \Gamma)$) are to the right of and above $\text{nearX}(v, \Gamma)$ (resp., $\text{nearY}(v, \Gamma)$). Moreover, from the planarity of Γ , it follows that $\text{label}(\text{nearX}(v, \Gamma)) \in \{\text{R}, \text{C}\} \setminus \{\text{label}(v)\}$ and $\text{label}(\text{nearY}(v, \Gamma)) \in \{\text{R}, \text{C}\} \setminus \{\text{label}(v)\}$. See Fig. 7c.

Observation 6. *Let v be an R- or a C-vertex of G^\rightarrow such that $\text{left}(v)$ and $\text{above}(v)$ exist. Let Γ be a drawing of G^\rightarrow such that there exists a vertex u for which (i) $x(u) \in [x(\text{left}(v)), x(\text{above}(v))]$, (ii) $y(u) \in [y(\text{left}(v)), y(\text{above}(v))]$, and (iii) $u, \text{prev}(u), \text{next}(u) \notin \{\text{left}(v), \text{above}(v)\}$. Let S be the set of all such vertices. Let $\text{maxY} = \max\{y(v) \mid v \in S\}$ and $\text{maxX} = \max\{x(v) \mid v \in S\}$.*

Then, $\text{nearX}(v, \Gamma)$ is the vertex in S such that $x(\text{nearX}(v, \Gamma)) = \max X$ and $y(\text{nearX}(v, \Gamma)) = \min\{y(v) \mid v \in S \wedge x(v) = \max X\}$. Similarly, $\text{nearY}(v, \Gamma)$ is the vertex in S such that $y(\text{nearY}(v, \Gamma)) = \min Y$ and $x(\text{nearY}(v, \Gamma)) = \max\{x(v) \mid v \in S \wedge y(v) = \min Y\}$. It follows from the definition that the neighbors of $\text{nearX}(v, \Gamma)$ (resp., $\text{nearY}(v, \Gamma)$) are to the left of and above $\text{nearX}(v, \Gamma)$ (resp., $\text{nearY}(v, \Gamma)$). Moreover, from the planarity of Γ , it follows that $\text{label}(\text{nearX}(v, \Gamma)) \in \{R, C\} \setminus \{\text{label}(v)\}$ and $\text{label}(\text{nearY}(v, \Gamma)) \in \{R, C\} \setminus \{\text{label}(v)\}$. See Fig. 7d.

We now give a reduction rule similar to Reduction Rule 2 for a path labeled CRC.

Reduction Rule 5. Suppose that there exists a path $P = (u_1, u_2, u_3, u_4, u_5)$ in G^\rightarrow such that $\text{label}(u_2) = C$, $\text{label}(u_3) = R$ and $\text{label}(u_4) = C$. Then, delete the vertex u_3 and the edges incident to it from G^\rightarrow and add a new path (u_2, u'_3, u_4) to G^\rightarrow . Moreover, assign $\text{label}(u_2) = F$, $\text{label}(u'_3) = C$, $\text{label}(u_4) = F$, $\text{weight}((u_2, u'_3)) = \text{weight}((u_3, u_4))$ and $\text{weight}((u'_3, u_4)) = \text{weight}((u_2, u_3))$. The labels of all the remaining vertices and the weights of all the remaining edges stay the same. Let $G_{\text{red}}^\rightarrow$ be the reduced graph.

Lemma 8. Reduction Rule 5 is safe.

Proof. The proof of the lemma follows similarly to the proof of Lemma 2. \square

We now give a lemma similar to Lemma 3 for a path labeled CRRC.

Lemma 9. Suppose that there exists a path $P = (u_1, u_2, u_3, u_4, u_5, u_6)$ in G^\rightarrow such that $\text{label}(u_2) = \text{label}(u_5) = C$ and $\text{label}(u_3) = \text{label}(u_4) = R$. For any drawing Γ of G^\rightarrow , there exists another drawing Γ' of G^\rightarrow whose bounding box is same as that of Γ such that $y(u_2) = y(u_5)$ in Γ' .

Proof. The proof of the lemma follows similarly to the proof of Lemma 3. \square

We now give a lemma similar to Lemma 4 for paths labeled CRRR or RRRC.

Lemma 10. Suppose that there exists a path $P = (u_1, u_2, u_3, u_4, u_5, u_6)$ in G^\rightarrow such that $\text{label}(u_2) = C$ and $\text{label}(u_3) = \text{label}(u_4) = \text{label}(u_5) = R$ (resp., $\text{label}(u_2) = \text{label}(u_3) = \text{label}(u_4) = R$ and $\text{label}(u_5) = C$). For any drawing Γ of G^\rightarrow , $y(u_2) < y(u_5)$ in Γ .

Proof. The proof of the lemma follows similarly to the proof of Lemma 4. \square

We now give reduction rules similar to Reduction Rule 3 for paths labeled CCCR, CRRR and RRRC.

Reduction Rule 6. *Suppose that there exists a path $P = (u_1, u_2, u_3, u_4, u_5, u_6)$ in G^\rightarrow such that $\text{label}(u_2) = \text{label}(u_3) = \text{label}(u_4) = \text{C}$ and $\text{label}(u_5) = \text{R}$. Then, delete the vertices u_3 and u_4 and the edges incident to them from G^\rightarrow and add a new path (u_2, u'_3, u_5) to G^\rightarrow . Moreover, assign $\text{label}(u_2) = \text{C}$, $\text{label}(u'_3) = \text{C}$, $\text{label}(u_5) = \text{F}$, $\text{weight}((u'_3, u_5)) = \text{weight}((u_3, u_4))$, $\text{weight}((u_6, \text{next}(u_6))) = \max\{\text{weight}((u_4, u_5)), \text{weight}((\text{next}(u_1), u_1))\}$, and $\text{weight}((u_2, u'_3)) = \max\{\text{weight}((u_2, u_3)) - \text{weight}((u_4, u_5)), 1\}$. The labels of all the remaining vertices and the weights of all the remaining edges stay the same. Let $G_{\text{red}}^\rightarrow$ be the reduced graph.*

Lemma 11. *Reduction Rule 6 is safe.*

Proof. The proof of the lemma follows similarly to the proof of Lemma 5. \square

Reduction Rule 7. *Suppose that there exists a path $P = (u_1, u_2, u_3, u_4, u_5, u_6)$ in G^\rightarrow such that $\text{label}(u_2) = \text{C}$ and $\text{label}(u_3) = \text{label}(u_4) = \text{label}(u_5) = \text{R}$. Then, delete the vertices u_3 and u_4 and the edges incident to them from G^\rightarrow and add a new path (u_2, u'_3, u_5) to G^\rightarrow . Moreover, assign $\text{label}(u_2) = \text{F}$, $\text{label}(u'_3) = \text{R}$, $\text{label}(u_5) = \text{R}$, $\text{weight}((u_2, u'_3)) = \text{weight}((u_3, u_4))$, $\text{weight}((\text{prev}(u_1), u_1)) = \max\{\text{weight}((u_2, u_3)), \text{weight}((\text{prev}(u_1), u_1))\}$, and $\text{weight}((u'_3, u_5)) = \max\{\text{weight}((u_4, u_5)) - \text{weight}((u_2, u_3)), 1\}$. The labels of all the remaining vertices and the weights of all the remaining edges stay the same. Let $G_{\text{red}}^\rightarrow$ be the reduced graph.*

Lemma 12. *Reduction Rule 7 is safe.*

Proof. The proof of the lemma follows similarly to the proof of Lemma 5. \square

Reduction Rule 8. *Suppose that there exists a path $P = (u_1, u_2, u_3, u_4, u_5, u_6)$ in G^\rightarrow such that $\text{label}(u_2) = \text{label}(u_3) = \text{label}(u_4) = \text{R}$ and $\text{label}(u_5) = \text{C}$. Then, delete the vertices u_3 and u_4 and the edges incident to them from G^\rightarrow and add a new path (u_2, u'_3, u_5) to G^\rightarrow . Moreover, assign $\text{label}(u_2) = \text{R}$, $\text{label}(u'_3) = \text{R}$, $\text{label}(u_5) = \text{F}$, $\text{weight}((u'_3, u_5)) = \text{weight}((u_3, u_4))$, $\text{weight}((u_6, \text{next}(u_6))) = \max\{\text{weight}((u_4, u_5)), \text{weight}((\text{next}(u_1), u_1))\}$, and $\text{weight}((u_2, u'_3)) = \max\{\text{weight}((u_2, u_3)) - \text{weight}((u_4, u_5)), 1\}$. The labels of all the remaining vertices and the weights of all the remaining edges stay the same. Let $G_{\text{red}}^\rightarrow$ be the reduced graph.*

Lemma 13. *Reduction Rule 8 is safe.*

Proof. The proof of the lemma follows similarly to the proof of Lemma 5. \square

We now give a reduction rule similar to Reduction Rule 4 for a path labeled CRRC.

Reduction Rule 9. *Suppose that there exists a path $P = (u_1, u_2, u_3, u_4, u_5, u_6)$ in G^\rightarrow such that $\text{label}(u_2) = \text{label}(u_5) = C$ and $\text{label}(u_3) = \text{label}(u_4) = R$. Then, delete the vertices u_3 and u_4 and the edges incident to them from G^\rightarrow and add a new edge (u_2, u_5) to G^\rightarrow . Moreover, assign $\text{label}(u_2) = \text{label}(u_5) = F$, $\text{weight}((u_2, u_5)) = \text{weight}((u_3, u_4))$ and $\text{weight}((\text{prev}(u_1), u_1)) = \max\{\text{weight}((u_2, u_3)), \text{weight}((\text{prev}(u_1), u_1))\}$. The labels of all the remaining vertices and the weights of all the remaining edges stay the same. Let $G_{\text{red}}^\rightarrow$ be the reduced graph.*

Lemma 14. *Reduction Rule 9 is safe.*

Proof. The proof of the lemma follows the proof of Lemma 6. \square